

AD-A263 220

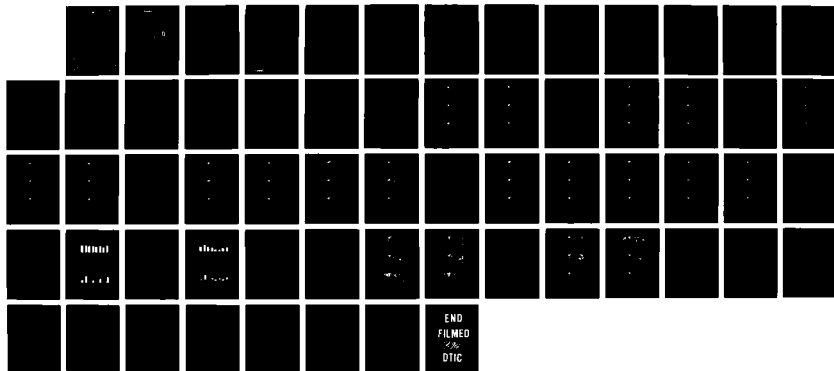
THE SEASONAL CYCLE DEPENDENCE OF TEMPERATURE
FLUCTUATIONS IN THE ATMOSPHERE(U) AIR FORCE INST OF
TECH WRIGHT-PATTERSON AFB OH B F TOBIN AUG 94

1/1

UNCLASSIFIED

AFIT/CI/CIA-94-103 XC-AFIT

NL



AD-A283 220

ON PAGE

Form Approved
OMB No. 0704-0188Public re
gatherin
collectio
Davis H

* 1 hour per response, including the time for reviewing instructions, searching existing data sources, collection of information. Send comments regarding this burden estimate or any other aspect of this collection of information, including suggestions for reducing this burden, to Washington Headquarters Services, Directorate for Information Operations and Reports, 1215 Jefferson Building, Washington, DC 20540, and to the Office of Management and Budget, Paperwork Reduction Project (0704-0188), Washington, DC 20503.

1. AG

3. REPORT TYPE AND DATES COVERED

4. TITLE AND SUBTITLE

The seasonal cycle Dependence of temperature
Fluctuations in the atmosphere

5. FUNDING NUMBERS

6. AUTHOR(S)

Bridget FRANCES TOBIN

7. PERFORMING ORGANIZATION NAME(S) AND ADDRESS(ES)

8. PERFORMING ORGANIZATION
REPORT NUMBER

9. SPONSORING / MONITORING AGENCY NAME(S) AND ADDRESS(ES)

DEPARTMENT OF THE AIR FORCE
AFIT/CI
2950 P STREET
WRIGHT-PATTERSON AFB OH 45433-776510. SPONSORING / MONITORING
AGENCY REPORT NUMBER

11. SUPPLEMENTARY NOTES

12a. DISTRIBUTION / AVAILABILITY STATEMENT

Approved for Public Release IAW 190-1
Distribution Unlimited
MICHEAL M. BRICKER, SMSgt, USAF
Chief Administration

12b. DISTRIBUTION CODE

13. ABSTRACT (Maximum 200 words)

14. SUBJECT TERMS

15. NUMBER OF PAGES

51

16. PRICE CODE

17. SECURITY CLASSIFICATION
OF REPORT18. SECURITY CLASSIFICATION
OF THIS PAGE19. SECURITY CLASSIFICATION
OF ABSTRACT

20. LIMITATION OF ABSTRACT

GENERAL INSTRUCTIONS FOR COMPLETING SF 298

The Report Documentation Page (RDP) is used in announcing and cataloging reports. It is important that this information be consistent with the rest of the report, particularly the cover and title page. Instructions for filling in each block of the form follow. It is important to *stay within the lines* to meet optical scanning requirements.

Block 1. Agency Use Only (Leave blank).

Block 2. Report Date. Full publication date including day, month, and year, if available (e.g. 1 Jan 88). Must cite at least the year.

Block 3. Type of Report and Dates Covered. State whether report is interim, final, etc. If applicable, enter inclusive report dates (e.g. 10 Jun 87 - 30 Jun 88).

Block 4. Title and Subtitle. A title is taken from the part of the report that provides the most meaningful and complete information. When a report is prepared in more than one volume, repeat the primary title, add volume number, and include subtitle for the specific volume. On classified documents enter the title classification in parentheses.

Block 5. Funding Numbers. To include contract and grant numbers; may include program element number(s), project number(s), task number(s), and work unit number(s). Use the following labels:

C - Contract	PR - Project
G - Grant	TA - Task
PE - Program Element	WU - Work Unit Accession No.

Block 6. Author(s). Name(s) of person(s) responsible for writing the report, performing the research, or credited with the content of the report. If editor or compiler, this should follow the name(s).

Block 7. Performing Organization Name(s) and Address(es). Self-explanatory.

Block 8. Performing Organization Report Number. Enter the unique alphanumeric report number(s) assigned by the organization performing the report.

Block 9. Sponsoring/Monitoring Agency Name(s) and Address(es). Self-explanatory.

Block 10. Sponsoring/Monitoring Agency Report Number. (If known)

Block 11. Supplementary Notes. Enter information not included elsewhere such as: Prepared in cooperation with...; Trans. of...; To be published in.... When a report is revised, include a statement whether the new report supersedes or supplements the older report.

Block 12a. Distribution/Availability Statement. Denotes public availability or limitations. Cite any availability to the public. Enter additional limitations or special markings in all capitals (e.g. NOFORN, REL, ITAR).

DOD - See DoDD 5230.24, "Distribution Statements on Technical Documents."
DOE - See authorities.
NASA - See Handbook NHB 2200.2.
NTIS - Leave blank.

Block 12b. Distribution Code.

DOD - Leave blank.
DOE - Enter DOE distribution categories from the Standard Distribution for Unclassified Scientific and Technical Reports.
NASA - Leave blank.
NTIS - Leave blank.

Block 13. Abstract. Include a brief (Maximum 200 words) factual summary of the most significant information contained in the report.

Block 14. Subject Terms. Keywords or phrases identifying major subjects in the report.

Block 15. Number of Pages. Enter the total number of pages.

Block 16. Price Code. Enter appropriate price code (NTIS only).

Blocks 17. - 19. Security Classifications. Self-explanatory. Enter U.S. Security Classification in accordance with U.S. Security Regulations (i.e., UNCLASSIFIED). If form contains classified information, stamp classification on the top and bottom of the page.

Block 20. Limitation of Abstract. This block must be completed to assign a limitation to the abstract. Enter either UL (unlimited) or SAR (same as report). An entry in this block is necessary if the abstract is to be limited. If blank, the abstract is assumed to be unlimited.

94-103

**THE SEASONAL CYCLE DEPENDENCE OF TEMPERATURE
FLUCTUATIONS IN THE ATMOSPHERE**

A Thesis

by

BRIDGET FRANCES TOBIN

Submitted to the Office of Graduate Studies of
Texas A&M University
in partial fulfillment of the requirements for the degree of

MASTER OF SCIENCE

August 1994

Accession For	
NTIS CRA&I	<input checked="" type="checkbox"/>
DTIC TAB	<input type="checkbox"/>
Unannounced	<input type="checkbox"/>
Justification	
By	
Distribution /	
Availability Codes	
Dist	Avail and/or Special
A-1	

Major Subject: Meteorology

94-25399
 6/85

94 8 11 103

**THE SEASONAL CYCLE DEPENDENCE OF TEMPERATURE
FLUCTUATIONS IN THE ATMOSPHERE**

A Thesis
by
BRIDGET FRANCES TOBIN

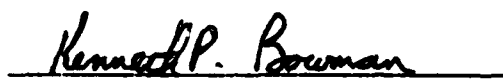
Submitted to Texas A&M University
in partial fulfillment of the requirements
for the degree of

MASTER OF SCIENCE

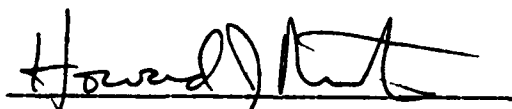
Approved as to style and content by:



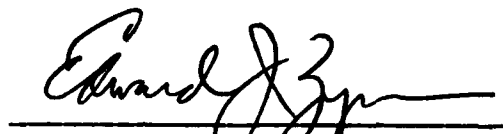
Gerald R. North
(Chair of Committee)



Kenneth P. Bowman
(Member)



Howard J. Newton
(Member)



Edward J. Zipser
(Head of Department)

August 1994

Major Subject: Meteorology

ABSTRACT

The Seasonal Cycle Dependence of Temperature Fluctuations in the Atmosphere. (August 1994)

Bridget Frances Tobin, B.S., Creighton University

Chair of Advisory Committee: Dr. Gerald R. North

The correlation statistics of meteorological fields have been of interest in weather forecasting for many years and are also of interest in climate studies. A better understanding of the seasonal variation of correlation statistics can be used to determine how the seasonal cycle of temperature fluctuations should be simulated in noise-forced energy balance models. It is shown that the length scale does have a seasonal dependence and will have to be handled through the seasonal modulation of other coefficients in noise-forced energy balance models. The temperature field variance and spatial correlation fluctuations exhibit seasonality with fluctuation amplitudes larger in the winter hemisphere and over land masses. Another factor contributing to seasonal differences is the larger solar heating gradient in the winter.

40 years of monthly mean surface data and 25 years of monthly mean 700mb and 500mb data is averaged over the

seasons. The spatial correlation of four northern hemisphere mid-latitude test sites, two ocean sites and two land sites, at the surface, at 700mb and at 500mb is examined for the winter, spring, summer and fall. The correlations between the different vertical levels and the variance of each level is also presented and examined.

ACKNOWLEDGEMENTS

I would like to thank the members of my committee, Drs. Gerald R. North, Kenneth P. Bowman and Howard J. Newton, for their assistance in developing and writing this thesis. Most of all, I would like to thank the chairman of my committee, whose advice and direction was most valuable in doing my research and writing this thesis.

In addition, I would like to thank Mark Stevens for his assistance in programming and every other aspect of this endeavour. I would also like to thank my fellow graduate students and all the professors in the Meteorology Department that have assisted me during my 2 years at Texas A&M.

TABLE OF CONTENTS

	Page
ABSTRACT	iii
ACKNOWLEDGEMENTS	v
TABLE OF CONTENTS	vi
LIST OF FIGURES	vii
INTRODUCTION	1
OBJECTIVES	4
DATA	5
SPATIAL CORRELATION AT DIFFERENT VERTICAL LEVELS . . .	9
CORRELATIONS BETWEEN VERTICAL LEVELS	31
VARIANCE	36
CONCLUSIONS	42
REFERENCES	49
VITA	51

LIST OF FIGURES

FIGURE	Page
1 The percentage of global surface area without data coverage from 1900 to 1990.	8
2 Spatial correlation of winter temperatures over North America.	10
3 Spatial correlation of spring temperatures over North America.	11
4 Spatial correlation of fall temperatures over North America.	13
5 Spatial correlation of summer temperatures over North America.	14
6 Spatial correlation of winter temperatures over Siberia.	16
7 Spatial correlation of spring temperatures over Siberia.	17
8 Spatial correlation of fall temperatures over Siberia.	18
9 Spatial correlation of summer temperatures over Siberia.	20
10 Spatial correlation of winter temperatures over the Pacific Ocean.	21
11 Spatial correlation of spring temperatures over the Pacific Ocean.	22
12 Spatial correlation of fall temperatures over the Pacific Ocean.	23
13 Spatial correlation of summer temperatures over the Pacific Ocean.	25
14 Spatial correlation of winter temperatures over the Atlantic	

FIGURE	Page
Ocean.	26
15 Spatial correlation of spring temperatures over the Atlantic Ocean.	27
16 Spatial correlation of fall temperatures over the Atlantic Ocean.	28
17 Spatial correlation of summer temperatures over the Atlantic Ocean.	29
18 Vertical correlations over North America.	32
19 Vertical correlations over Siberia.	32
20 Vertical correlations over the North Pacific.	34
21 Vertical correlations over the North Atlantic.	34
22 Variance of winter temperatures.	37
23 Variance of spring temperatures.	38
24 Variance of fall temperatures.	40
25 Variance of summer temperatures.	41

INTRODUCTION

The spatial correlation of meteorological fields has been of interest in weather forecasting for many years. It is used in optimal interpolation schemes in the preparation of input for numerical weather forecasts since data are collected at irregularly positioned stations and model input is on a regular grid. The correlation structures are also of interest in climate studies. A better understanding of the seasonal variation of correlation statistics can be used to determine how the seasonal cycle of surface temperature fluctuations should be simulated in noise-forced energy balance models (nfEBMs). If the length scale of the fields does not have a seasonal variation, it may be possible to include seasonal modulation of the fluctuations exclusively in the forcing noise. If the length scale does have a seasonal dependence, the fluctuations will have to be handled through the seasonal modulation of system parameters, such as the diffusion coefficient.

Until recently, most of what is known concerning interannual and interdecadal variability in the temperature fields has been limited to the analysis of the horizontal structure of surface air temperature records for land stations. This study is an exploratory data analysis of monthly mean temperature data averaged into seasons. It will concentrate on the patterns of spatial correlation of temperature at the surface, 700mb and 500mb, the differences in the spatial correlation at different test sites, the correlation between the surface and 700mb, the surface and 500mb, and 700mb and

The thesis style is that of the *Monthly Weather Review*.

500mb and the variance of the temperature field at these three levels. Earlier studies of temperature fields focus on global surface temperature (Hansen and Lebedeff, 1987), on temporal trends in surface temperature (Jones, 1988), the variance of northern hemisphere surface temperature by seasons over time, but not over space (Jones and Briffa, 1992). Kim and North (1991) compared the results of noise-forced energy balance models with the observational results of the same surface data set used in this paper, but did not include upper level data.

The autocorrelation length scale found in annual averaged observational surface temperature data is about 1500km (Hansen and Lebedeff, 1987; Kim and North, 1991). 1500km is the inherent length scale for long term averages in noise-forced energy balance models (North, 1982). It also happens to be the characteristic size for the synoptic scale features that are prominent on daily weather maps. This latter is probably due to the corresponding size of the Rossby radius of deformation (Hess, 1959). The climate (time averaged data) length scale is not solely determined by dynamical considerations but seems to be dependent on radiation damping as well.

It is interesting to see if this is a property exclusively of the surface temperature. If one takes disks of 1500km radius and covers the earth, about 65 are required. This implies there are about 65 statistically independent regions on the earth with respect to low frequency surface temperature fluctuations (Hardin and Upson, 1993). If the correlation lengths are significantly larger in one season than in the other, it may be possible to use

fewer than 65 statistically independent regions to cover the earth during that season. At the same time, the correlation areas seem to be largest in the more variable seasons. This coincidence suggests that a compensation occurs making the sampling errors seasonally invariant. Currently it is unclear whether the present distribution of surface temperature gauges is adequate for estimation of large scale temperature features and this uncertainty has resulted in questions about whether temperature anomalies on a hemispheric or global basis can be inferred from conventional data.

The surface temperature field variance and spatial correlation do exhibit seasonality. Variability of hemispheric surface temperatures is largest in the winter, followed by spring, fall and summer (Jones and Bradley, 1992). Fluctuation amplitudes are larger in the winter hemisphere because there is more potential for atmospheric flow instabilities. The fluctuations are also larger over land masses. The different effective heat capacities of land and ocean mixed layer are partially accountable for the larger fluctuations in the winter hemisphere. The heat capacity of the water is about three times that of dry soil and double that of wet soil. Therefore, land surfaces heat and cool much quicker than oceans. Furthermore, turbulent mixing causes the effective heat capacity over ocean areas to be another order of magnitude larger. Heat storage in the oceans causes them to be warmer in winter and cooler in summer than land, ignoring the effects of ocean currents (Barry and Chorley, 1982). Finally, the solar heating gradient is larger in winter than in summer. These results combine to cause larger transient thermal gradients in the winter and the increased potential for dynamic instability.

OBJECTIVES

The research goal of this study is to expand current knowledge of the correlation statistics of seasonally averaged temperature fields at the surface, 700mb and 500mb. To achieve this goal, this study examines four representative sites in the Northern Hemisphere mid-latitudes. How the spatial correlations vary seasonally for the four different test sites and how the pattern of spatial correlation changes vertically through the troposphere at each of these test sites will be examined. The correlation between the different vertical levels are also examined for an area surrounding each test site that corresponds to the $.368$ ($1/e$) correlation distance. Finally, the variance over the northern hemisphere for the seasonally averaged temperature fields is also presented.

DATA

The primary data for this study consist of two temperature data sets. The surface data is from the United Kingdom global surface temperatures prepared and maintained by NCAR. Using the most comprehensive climate data Jones et al. (1986) and Jones (1988) have produced a grid-point data set of surface air temperature anomalies for each month since January 1851. To overcome the irregular distribution of individual stations, the basic station data has been interpolated to a grid. Air temperatures are used over land and water temperatures over ocean. This data set combines the grid-point land and grid-box marine data into a $5^{\circ}\text{X}5^{\circ}$ grid box data set. Where collocated land and marine grid data occur, the resulting value in a grid box is the average of the land and marine components. The temperature data are expressed as departures from the common reference period mean of 1951-70 to enable interpolation to be easily achieved. Absolute mean temperatures recorded at neighboring stations will vary because of factors such as site evaluation and techniques used to calculate mean monthly temperature. Interpolation of data in absolute values will also be affected by these problems and by varying station numbers. The use of anomaly values from a common reference period overcomes these problems. A consequence of this procedure is that average hemispheric temperatures are only calculated in relative and not in absolute terms. The marine data is the result of both marine air and sea surface temperature measurements taken by ships. The marine air temperatures are subject to biases induced by the overheating of poorly located thermometers by solar insolation. These

biases have changed with time as ships have increased in size (height above sea surface) and speed. Marine data are also subject to biases induced by the different methods of sampling the sea water. Before World War II the sea water was collected in an uninsulated canvas bucket. There was also a delay between sampling and measuring the temperature. Though the delay was only a few minutes, it was enough time for the water in the bucket to cool slightly by evaporative means. Since World War II most readings have been made in the intake pipes through which sea water is taken on board ships to cool the engines. The bucket measurements are cooler by 0.3-0.7°C. A method has been developed to correct for the uninsulated buckets. The coverage of SST measurements is largely determined by merchant shipping routes. In most analyses (Jones and Wigley, 1990; Jones et al., 1991; Folland et al., 1990) temperatures over the ocean can be estimated using sea surface temperature anomalies providing improved spatial coverage. Although the difference between air and sea temperatures can be up to 6-8°C in absolute terms, the two marine sets are in excellent agreement in anomaly terms. Sea surface temperature anomalies are, therefore, an excellent surrogate for marine air temperature anomalies (Jones and Briffa, 1992). Data is available from 85°N to 65°S on a 5° grid for January 1851 through April 1990.

The upper air data is also prepared and maintained by NCAR and was produced by splicing together several different grids from different analysis routines and interpolating them onto a common grid. Data is available for the Northern Hemisphere only, starting at 20°N. The sampling rate is twice daily,

at 00Z and 12Z. The 700mb temperature data is available for January 1963 through September 1993. The 500mb temperature data starts in January 1964 and ends in September 1993.

For this study, 40 years of surface data will be examined, starting in 1950 and ending in 1989. Prior to 1950, up to 60% of global surface area was without data coverage which is the primary motivation for only examining data after that time (Fig. 1). 25 years of upper air data will be examined, starting in 1964 and ending in 1988. The surface data grid is from 87.5°S to 87.5°N and 2.5°E to 357.5°E. The upper air data grid is from 0°N to 90°N and 5°E to 355°E. To account for the grid differences when correlating the surface and upper air data, an average will be taken over an equal number of grid-points. All examination of data will be done as seasonal averages of monthly means. Seasons are taken to be December, January, February (DJF) for winter, March, April, May (MAM) for spring, June, July, August (JJA) and September, October, November (SON) for fall. This study examines four representative sites in the Northern Hemisphere mid-latitudes. The locations include two land areas, one in central North America (37.5°N, 262.5°E) and one in central Asia (52.5°N, 92.5°E), and two ocean locations, an area over the Pacific (37.5°N, 212.5°E) and an area over the North Atlantic (52.5°N, 332.5°E). At the 700mb and 500mb levels the test sites will be 50°N; 90°E; 40°N, 260°E; 40°N, 210°E; and 50°N, 330°E. These test sites are the four of the six points studied in Kim and North's study of second moment statistics from a noise forced energy balance model (1991).

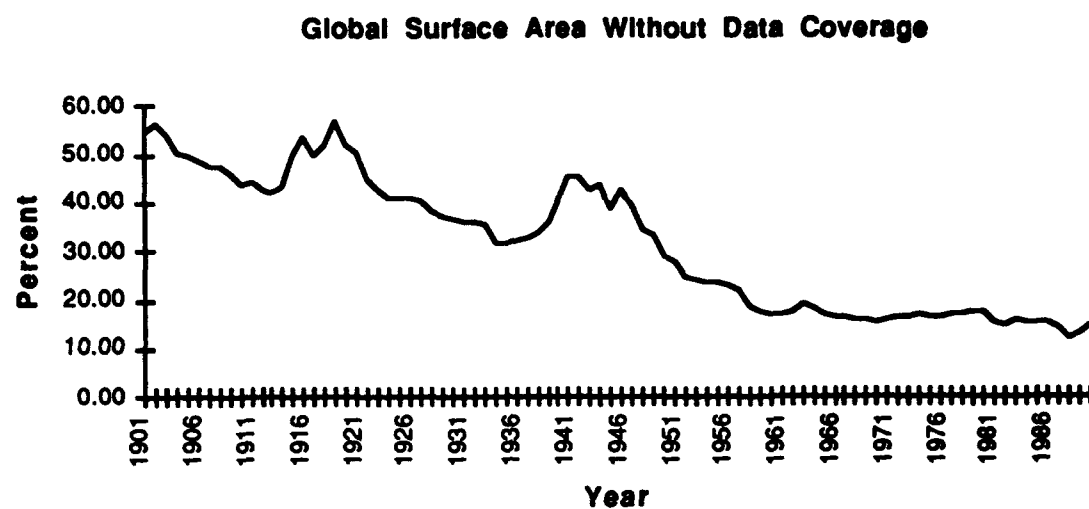


FIG. 1. The percentage of global surface area without data coverage from 1900 to 1990.

SPATIAL CORRELATION AT DIFFERENT VERTICAL LEVELS

The spatial correlation pattern over central North America for the winter season (Fig. 2) is concentrated around the test site at the surface . The west-east boundaries are the Rocky Mountains (247.5°E) and the east coast (292.5°E). The north-south borders are the southwest coast of the Hudson Bay (57.5°N) and the Gulf Coast (32.5°N). Small correlations are also apparent over the central Atlantic and over the Tibetan Plateau and a barely discernible correlation exists over Scandinavia. At 700mb , the correlation pattern exhibits the same size over the North American continent, but the pattern exhibits elongation to the east and a correlation maximum exists over the Atlantic that is much stronger than it was at the surface. A third correlation maximum is centered in an area east of Scandinavia and west of the Ural Mountains. The 500mb correlation pattern is essentially the same as the 700mb pattern but is not as strong. All three correlation areas are vertically stacked. The correlation is apparent at all three levels and the pattern is strongest at 700mb.

In the spring (Fig. 3), the next most variable season, the spatial correlation around the test site at the surface is much smaller, with much less north-south extent. There are no other areas of correlation at the surface. At 700mb, the spatial correlation immediately around the test site includes the same amount of area as at the surface, but a second area has become apparent over Greenland, a small area is visible off the east coast of China and a well defined area exists over the North Pacific. At 500mb the spatial correlation around the test point is larger and exhibits some elongation to the

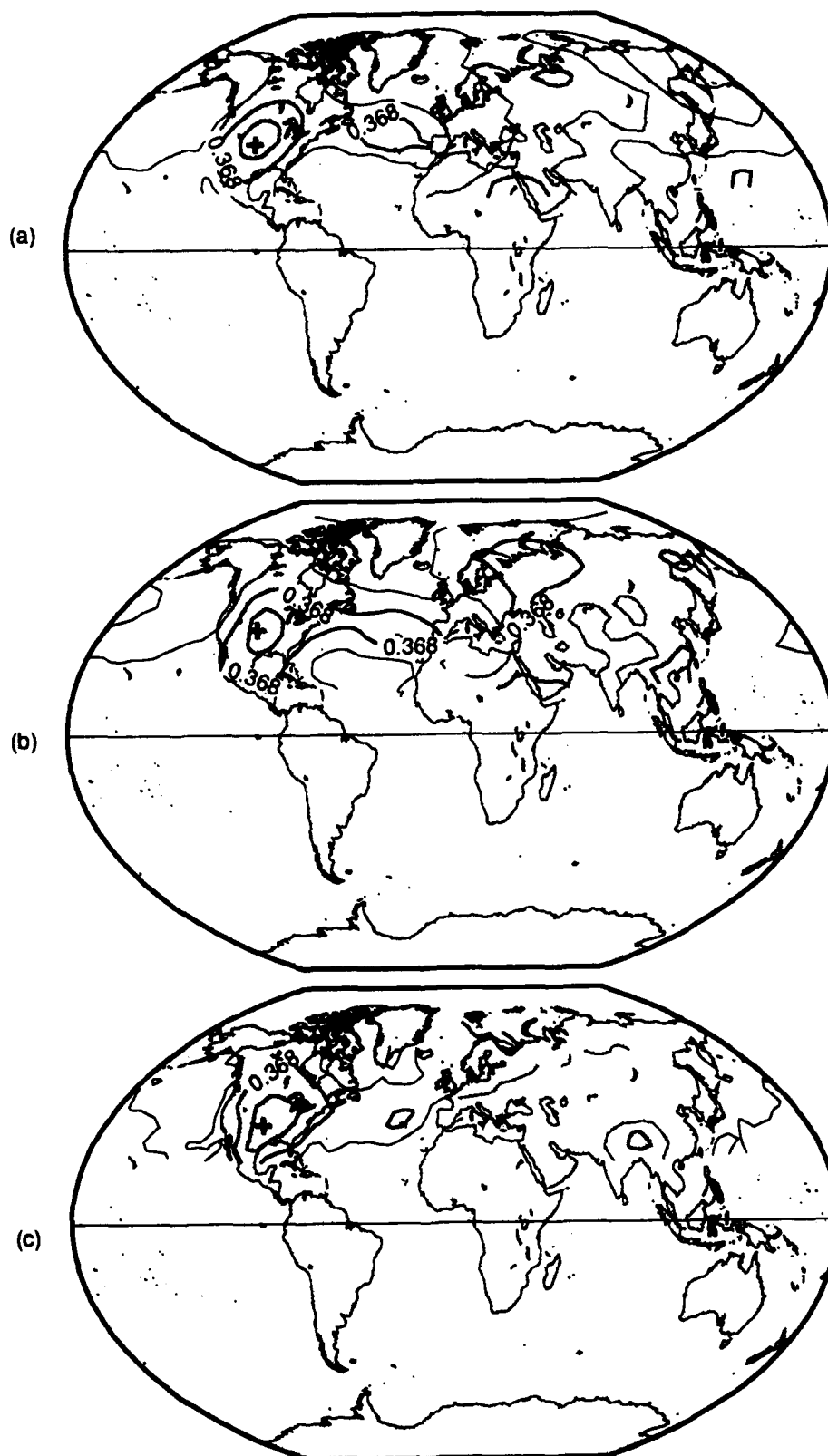


FIG. 2. Spatial correlation of winter temperatures over North America. (a) 500mb data at $260^{\circ}\text{E}, 40^{\circ}\text{N}$ for 1964 to 1988. (b) 700mb data at the same point for the same time. (c) Surface data at $262.5^{\circ}\text{E}, 37.5^{\circ}\text{N}$ for 1950-1989.

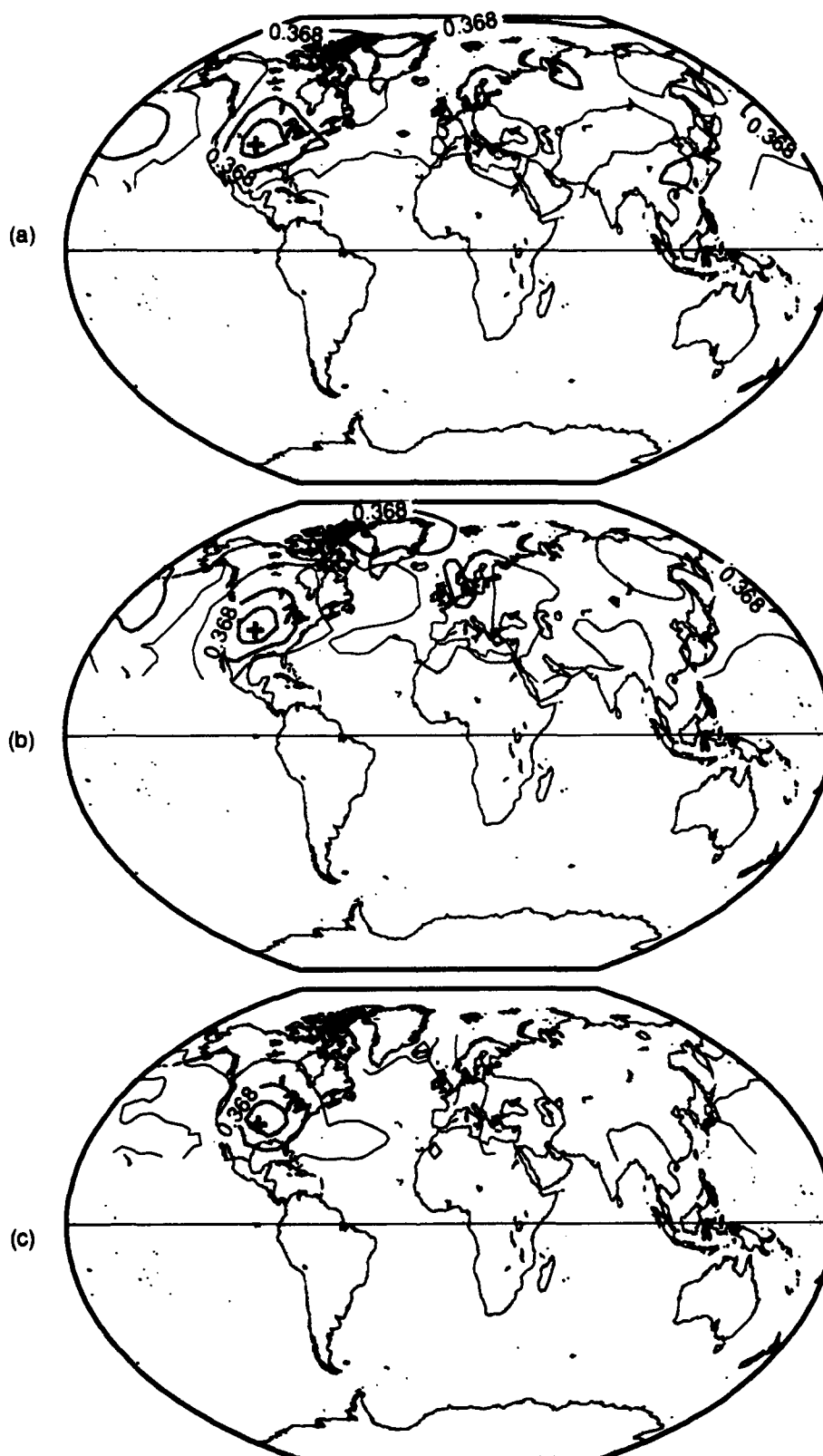


FIG. 3. Spatial correlation of spring temperatures over North America. (a) 500mb data at 260°E, 40°N for 1964 to 1988. (b) 700mb data at the same point for the same time. (c) Surface data at 262.5°E, 37.5°N for 1950-1989.

east, and the area over the North Pacific is larger and also exhibits some elongation to the east. The correlation over Greenland is unorganized and correlation is now apparent over the entire Arctic region. The spatial correlation at the test site continues to be vertically stacked. The North Pacific correlation is also stacked and organized at the 500mb level.

At the surface the fall spatial correlation includes more area around the test site than in the winter or the spring (Fig. 4). The east-west orientation is the same as in the winter and in the spring, but the area is elongated in the north-south, with the northernmost area north of the Hudson Bay. Another center is visible at the surface over Siberia. At 700mb the correlation around the test site is more compact, in fact, it is very similar to the spring 700mb correlation. The 700mb correlation also exhibits waves, with a correlation maximum over the Atlantic and the east coast of Spain and a large area of correlation over Siberia. The 500mb correlation exhibits waves in the same areas. As in the winter case these correlations are vertically stacked, barely discernible at the surface and most readily apparent at the 700mb level.

The summer season is the least variable season. At the surface, the spatial correlation is much smaller around the test site than in any other season and is elongated slightly to the north (Fig. 5). A second unorganized area is located over the Pacific coast of south China. The upper level correlations are completely unorganized, with numerous waves over the entire area of available data.

The second test site examined is in Siberia on the larger of the two land areas. As in North America, the area around the test site exhibits similar

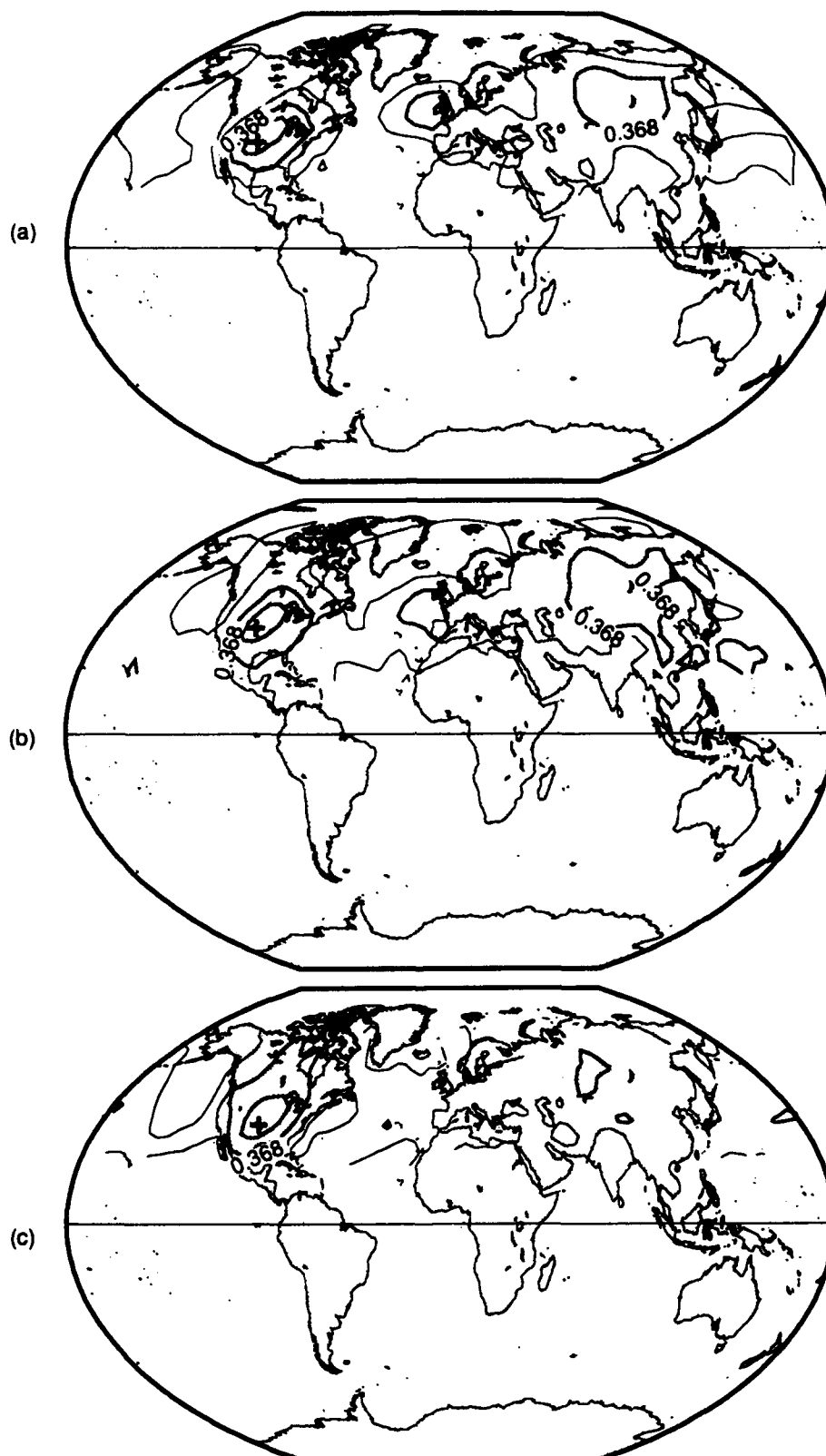


FIG. 4. Spatial correlation of fall temperatures over North America. (a) 500mb data at 260°E, 40°N for 1964 to 1988. (b) 700mb data at the same point for the same time. (c) Surface data at 262.5°E, 37.5°N for 1950-1989.

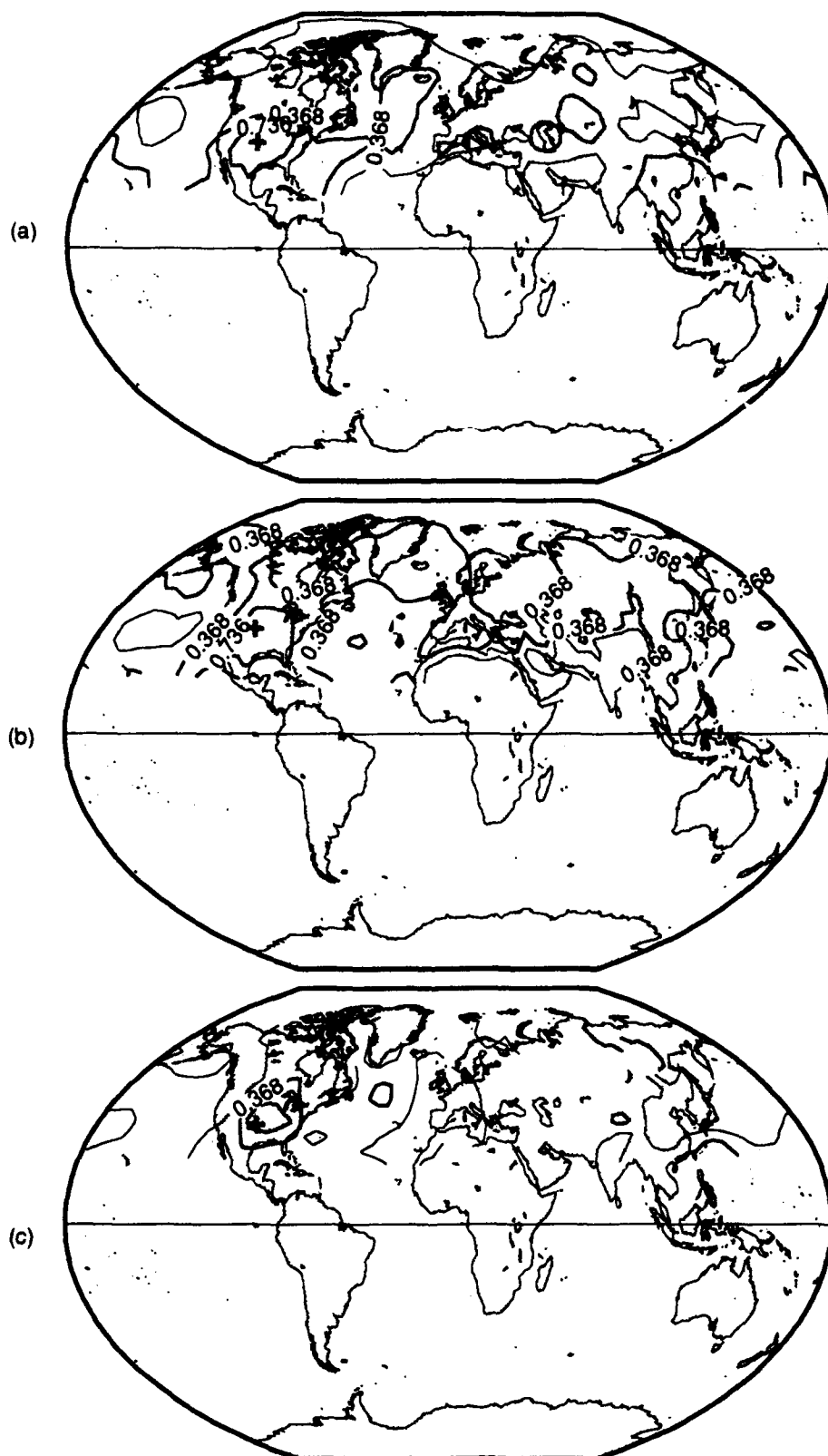


FIG. 5. Spatial correlation of summer temperatures over North America. (a) 500mb data at 260°E, 40°N for 1964 to 1988. (b) 700mb data at the same point for the same time. (c) Surface data at 262.5°E, 37.5°N for 1950-1989.

correlation at all three levels during the winter (Fig. 6). The largest areal extent at this test site occurs at the surface, in contrast with the North American case, which had the largest area at 700mb. Other areas of correlation are present in the field, an area north of Alaska, a small area off the west coast of North America and a smaller area over eastern Greenland are present. These areas of correlation don't extend to the surface in all areas. As in the previous case, the pattern is best seen at 700mb.

In the spring the correlation area is smaller than was the case in the winter around the test site (Fig. 7). As in the winter case there are additional areas with one over northern Europe, another in the central Atlantic and one in the Pacific. These subsequent areas do not extend to the 700mb level. At 700mb, there is are areas in Texas, over northern Greenland and over the Bering Strait. This pattern does not extend to the 500mb level. At 500mb the test site correlation is stretched to the east and the waves over Europe and the Pacific are again apparent.

The most organized wave pattern for this test site occurs in the fall (Fig. 8). The correlation around the test site is nicely stacked at all three levels, is more compact at the upper levels and slightly elongated to the east at 500mb. A second correlation area is located in the Atlantic, off the coast of the United Kingdom, and a third area is over the southeast coast of North America. These areas are apparent at all three levels and largest at the 500mb level.

The summer spatial correlation at the test site is very small at the surface with a second small area located in the North Pacific, just south of the

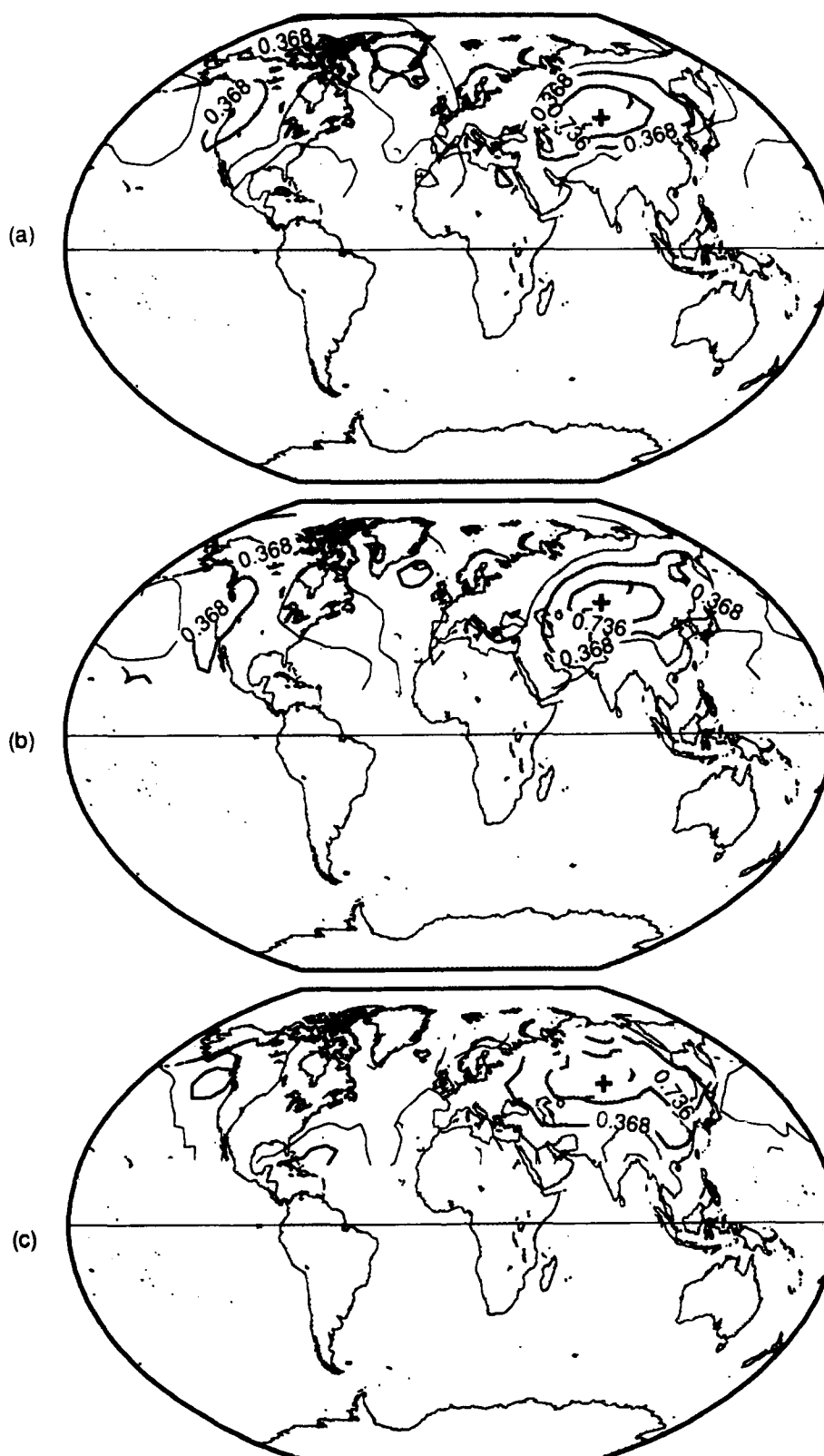


FIG. 6. Spatial correlation of winter temperatures over Siberia. (a) 500mb data at 90°E, 50°N for 1964 to 1988. (b) 700mb data at the same point for the same time. (c) Surface data at 92.5°E, 52.5°N for 1950-1989.

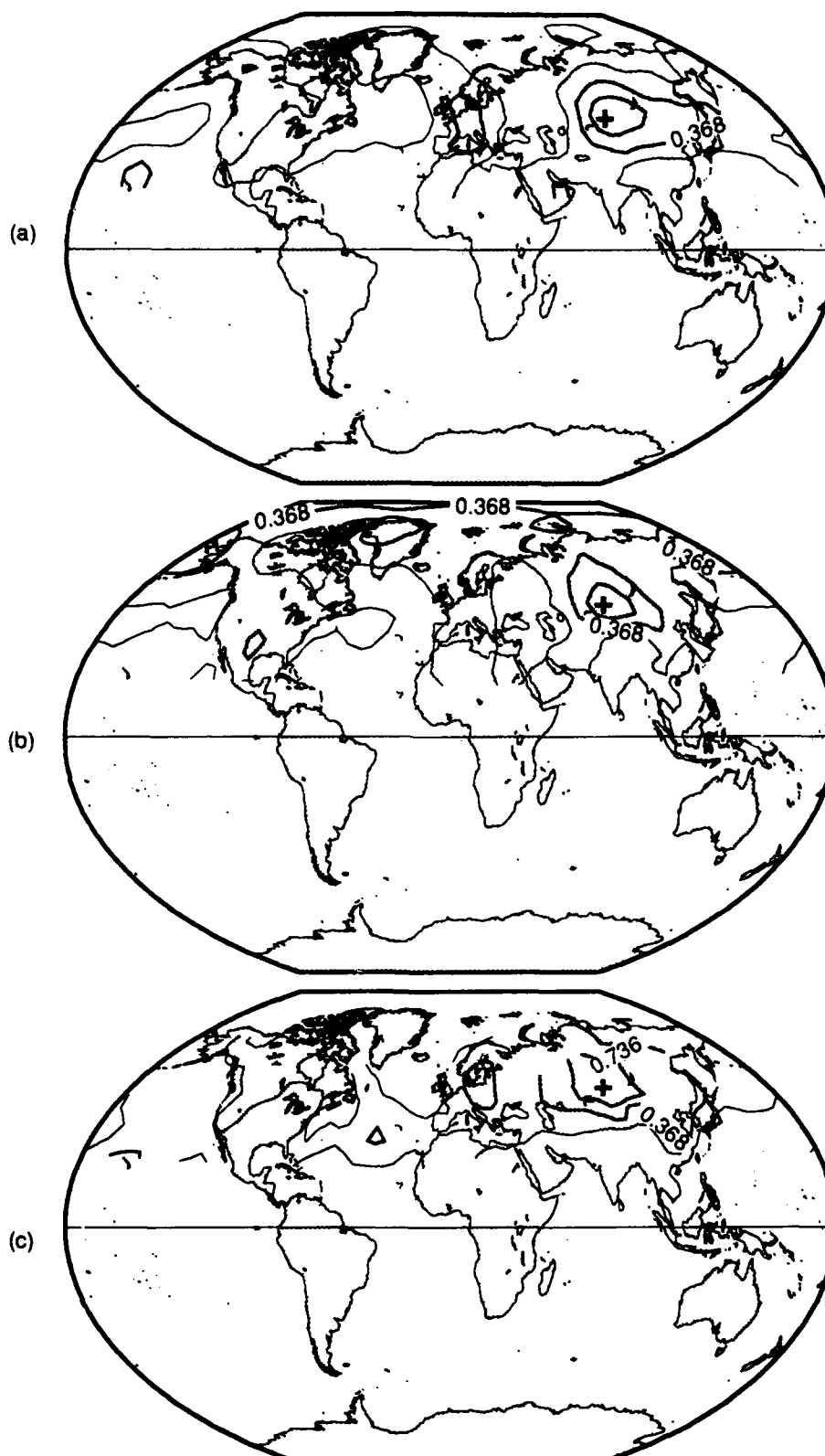


FIG. 7. Spatial correlation of spring temperatures over Siberia. (a) 500mb data at 90°E, 50°N for 1964 to 1988. (b) 700mb data at the same point for the same time. (c) Surface data at 92.5°E, 52.5°N for 1950-1989.

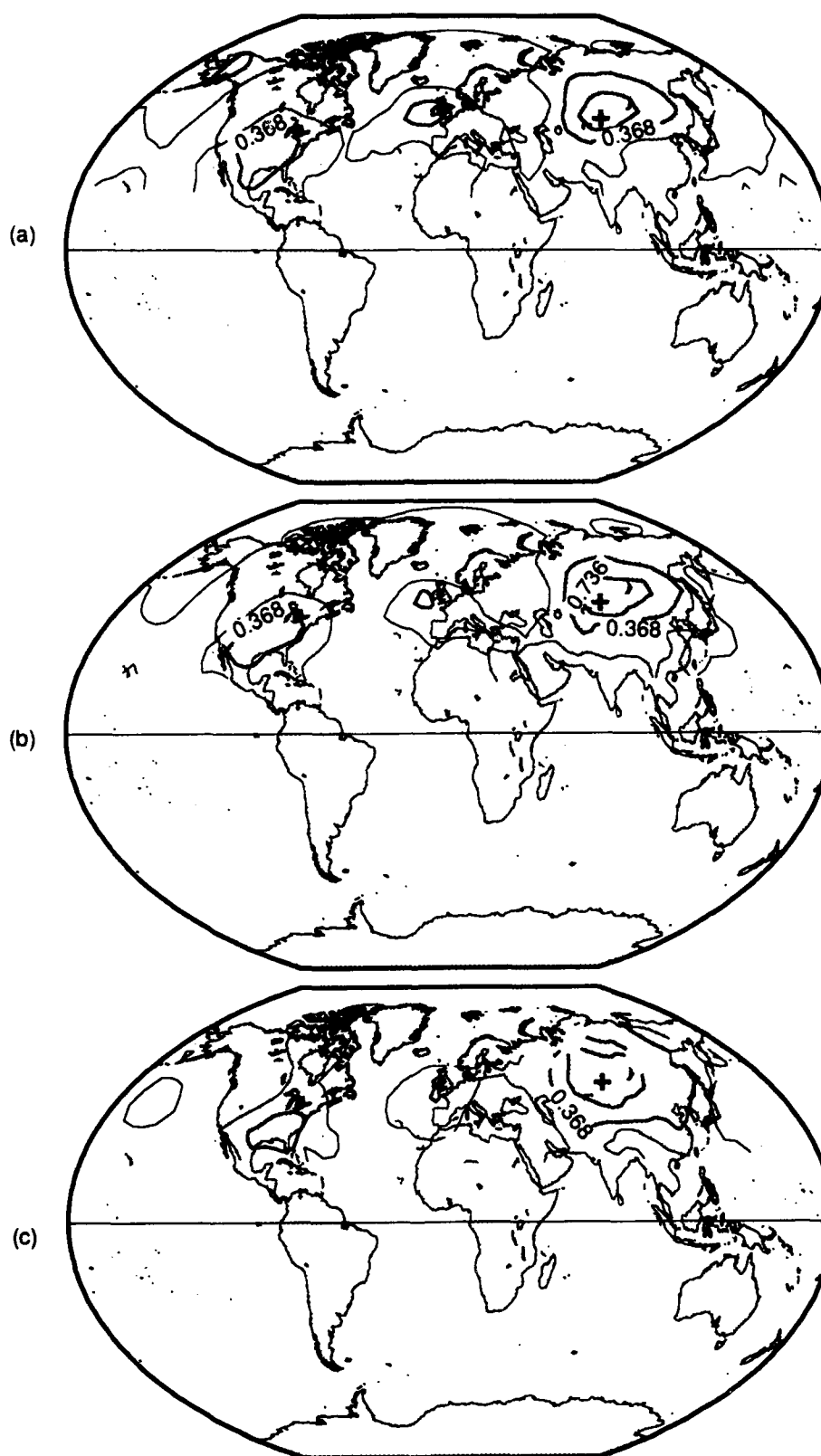


FIG. 8. Spatial correlation of fall temperatures over Siberia. (a) 500mb data at 90°E, 50°N for 1964 to 1988. (b) 700mb data at the same point for the same time. (c) Surface data at 92.5°E, 52.5°N for 1950-1989.

Aleutian islands (Fig. 9). The 700mb pattern is very unorganized, with correlations throughout the area of data coverage. The 500mb area at the test site resembles the area at the surface. The 500mb pattern is disorganized but is mostly confined to the Eurasian continent.

In the winter, over the North Pacific, the spatial correlation is confined to the North Pacific, except at the surface (Fig. 10). At the surface a small area of correlation is located over the southeastern coast of the United States. Unlike the land regions previously examined, the correlation area is not significantly larger at the surface than at other levels. In the spring the test site correlation is smaller at all three levels than it was in the winter and is significantly larger at the surface (Fig. 11) than at the upper levels. The second area over the North American southeast again exists but has moved to the west and now extends vertically to both 700mb and 500mb. The correlation over the North American southeast is largest at the 500mb level. There are also several other areas of correlation at 500mb, one west of the Gibraltar Strait, one over Greenland and one west of the Ural Mountains.

The fall spatial correlation is much smaller at all three levels around the test site with the largest area at 700mb (Fig. 12). The only other surface correlation is over the Pacific coast of Eurasia. At 700mb, there are three additional areas of correlation. The area over the southeastern United States is again apparent. Two more areas are apparent at 700mb, one over the United Kingdom and one over northern Siberia. At 500mb the area over southeast North America is much weaker, the Siberian area is much smaller and the United Kingdom area has disappeared. During the Summer, the test site spatial correlation at the surface is once again large (Fig. 13). At 700mb,

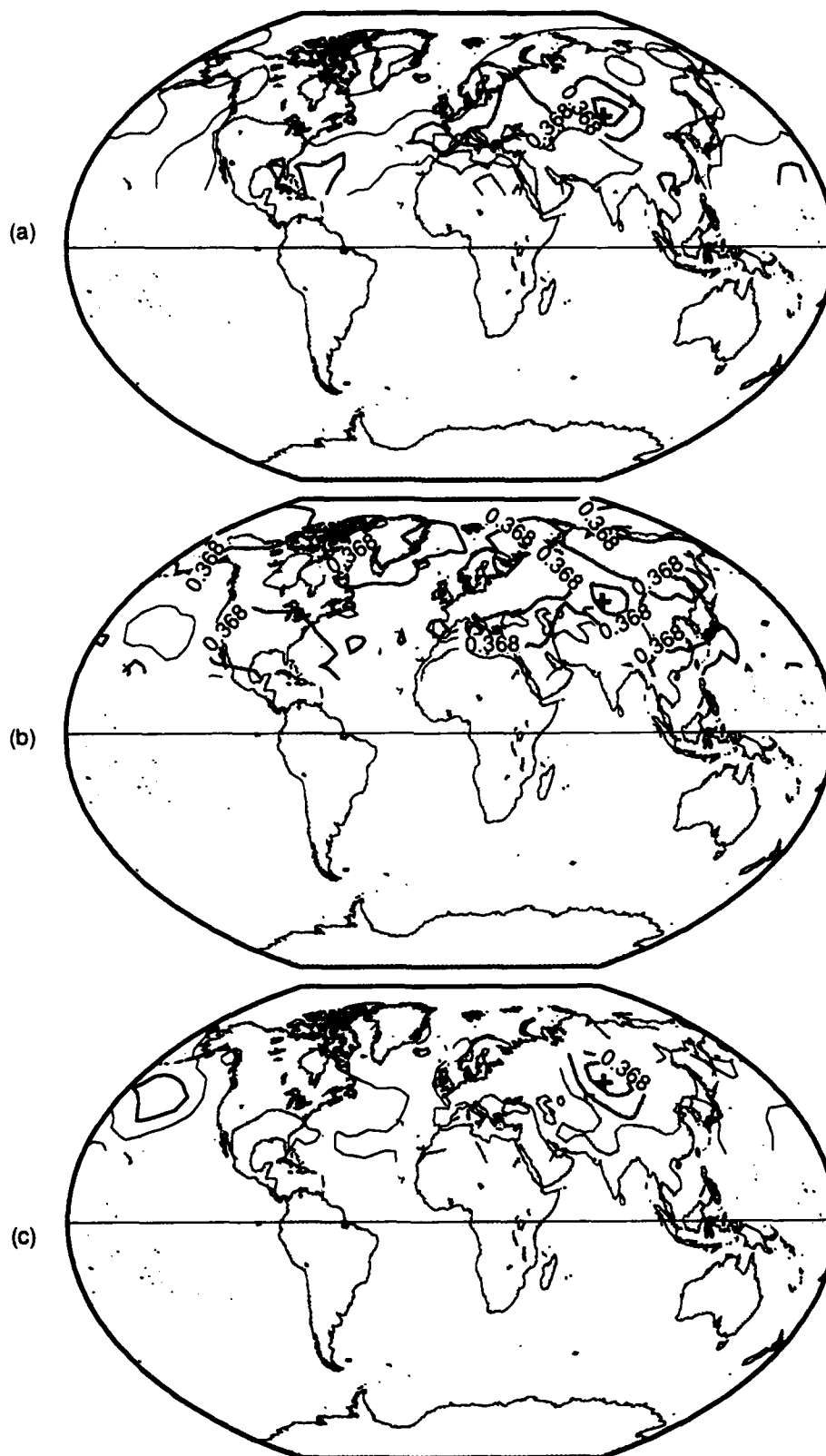


FIG. 9. Spatial correlation of summer temperatures over Siberia. (a) 500mb data at 90°E, 50°N for 1964 to 1988. (b) 700mb data at the same point for the same time. (c) Surface data at 92.5°E, 52.5°N for 1950-1989.

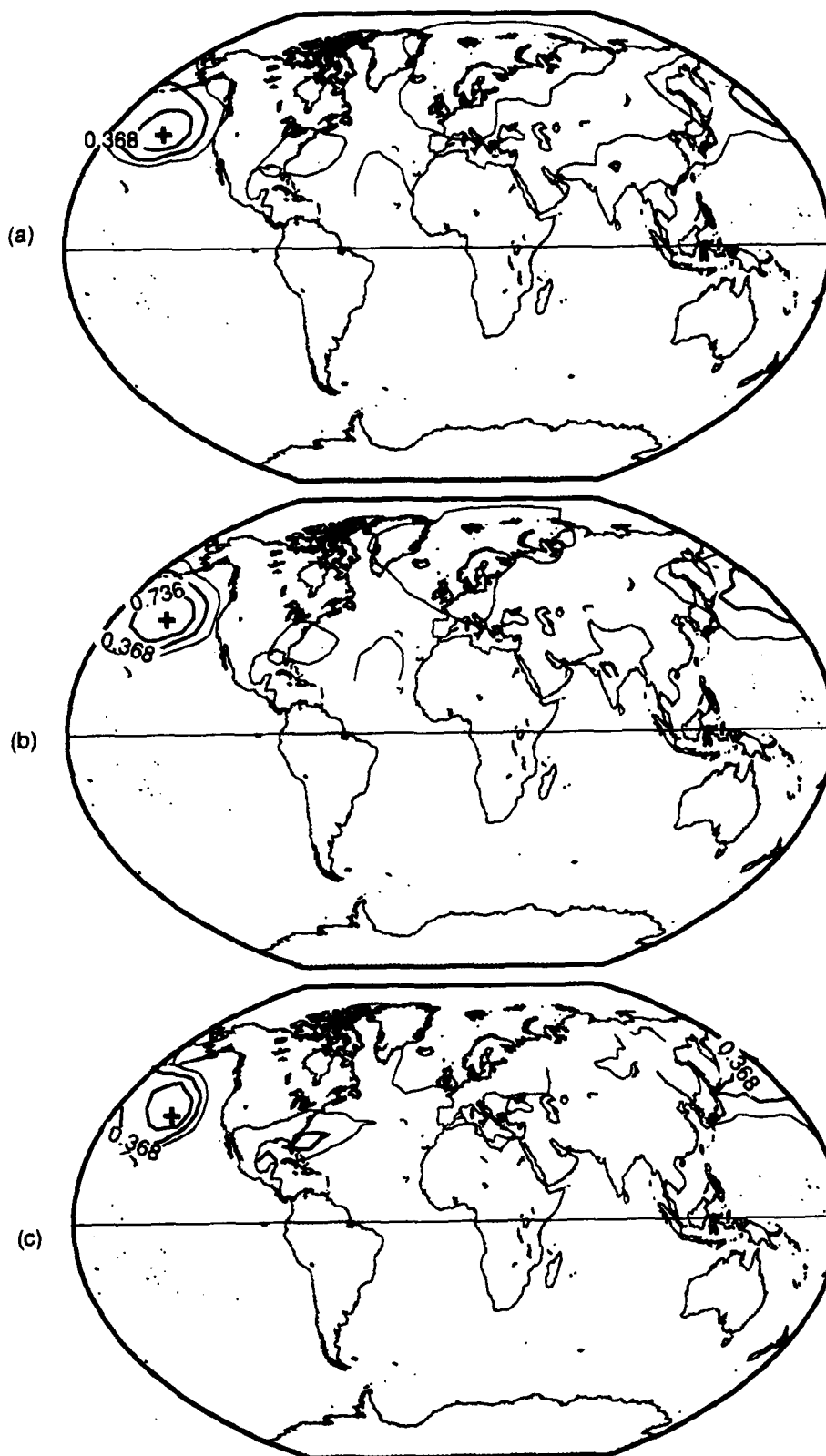


FIG. 10. Spatial correlation of winter temperatures over the Pacific Ocean. (a) 500mb data at 210°E, 40°N for 1964 to 1988. (b) 700mb data at the same point for the same time. (c) Surface data at 212.5°E, 37.5°N for 1950 to 1989.

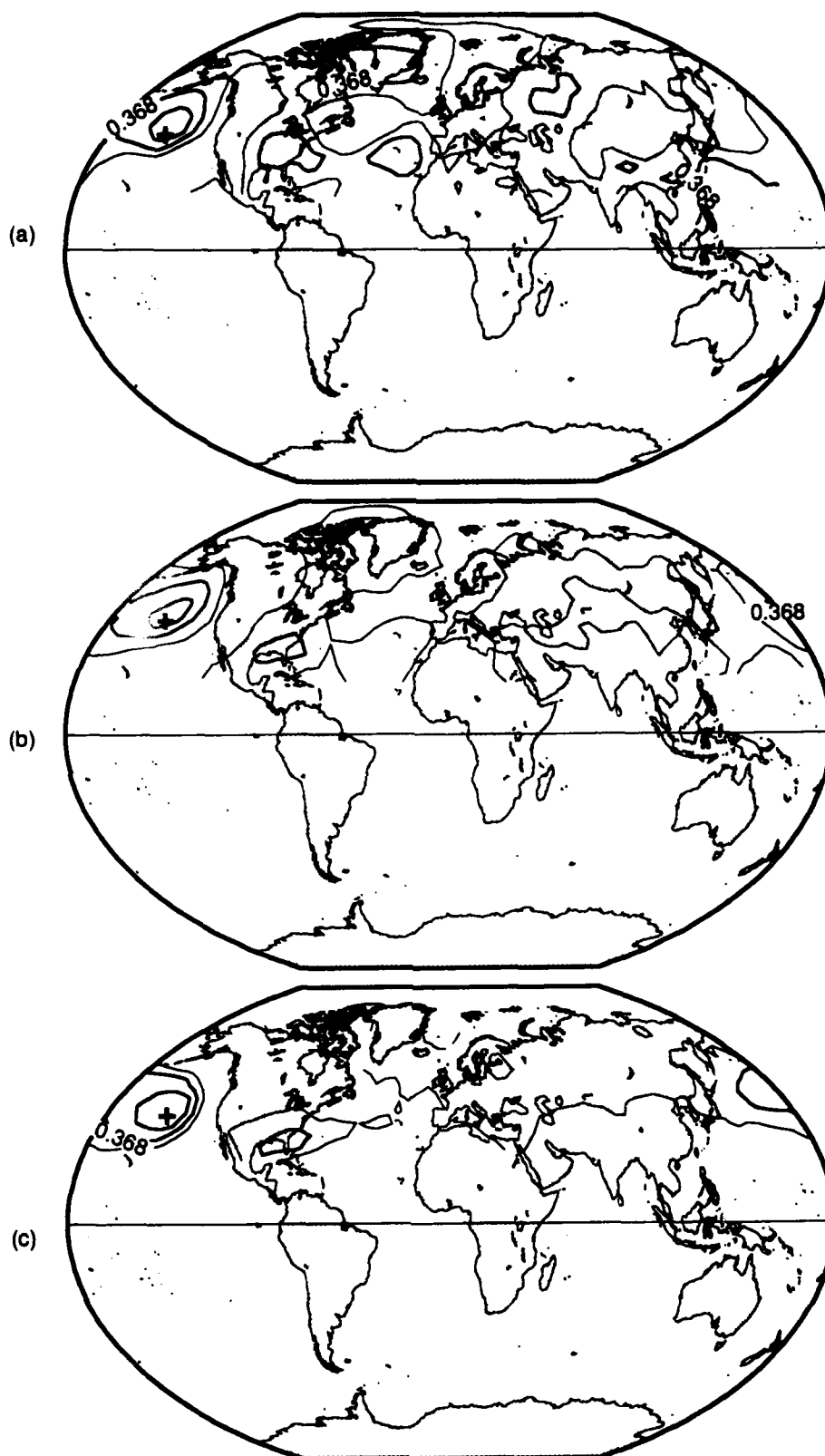


FIG. 11. Spatial correlation of spring temperatures over the Pacific Ocean. (a) 500mb data at 210°E, 40°N for 1964 to 1988. (b) 700mb data at the same point for the same time. (c) Surface data at 212.5°E, 37.5°N for 1950 to 1989.

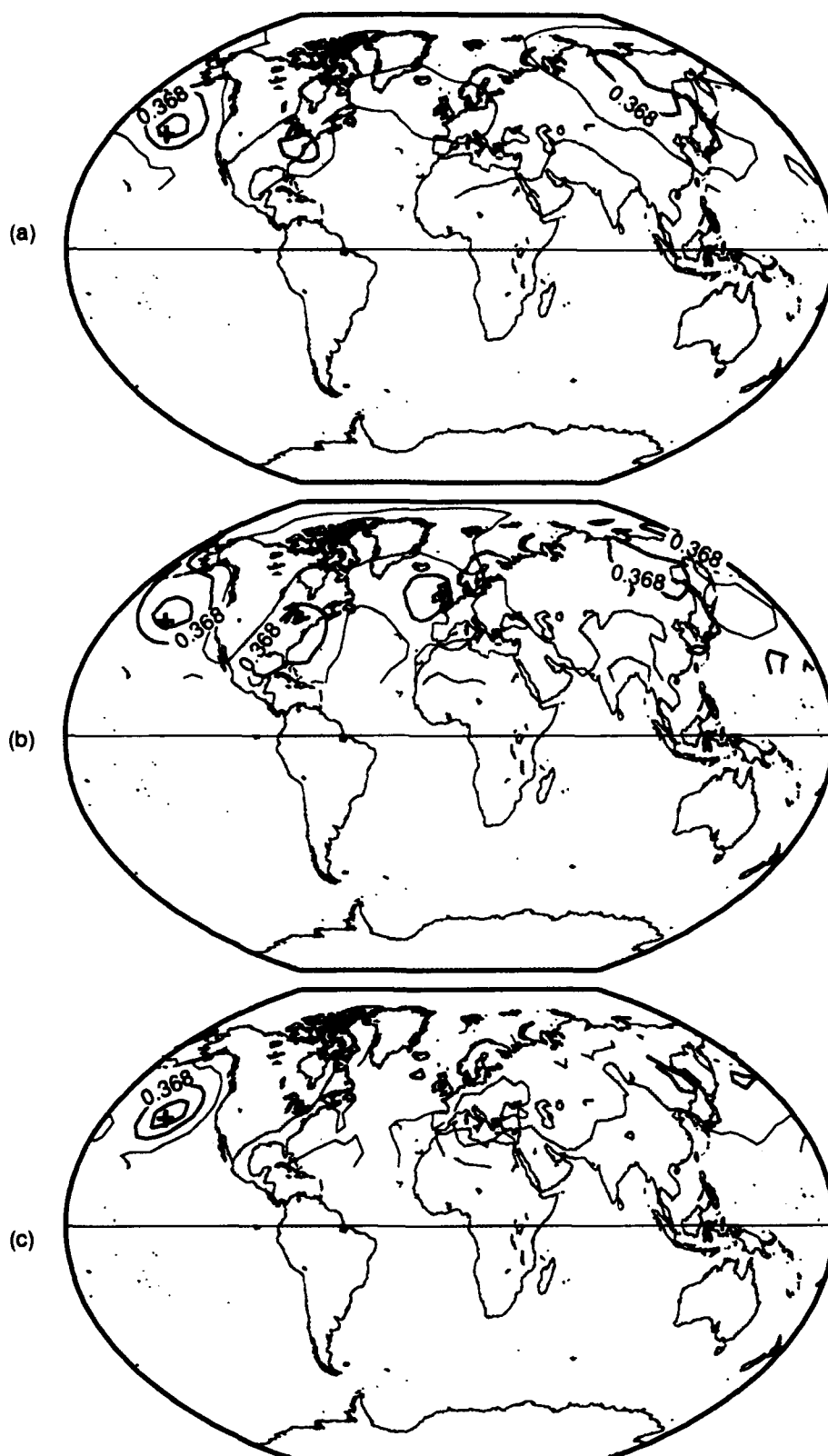


FIG. 12. Spatial correlation of fall temperatures over the Pacific Ocean. (a) 500mb data at $210^{\circ}\text{E}, 40^{\circ}\text{N}$ for 1964 to 1988. (b) 700mb data at the same point for the same time. (c) Surface data at $212.5^{\circ}\text{E}, 37.5^{\circ}\text{N}$ for 1950 to 1989.

as with the other test sites in the summer, the pattern is unorganized and covers the entire hemisphere. At 500mb only one area outside the test site area, in the South Atlantic, exhibits correlation.

The final test site is over the North Atlantic ocean. In the winter the spatial correlation at the surface is primarily around the test site, with another small area in the central Pacific (Fig. 14). At 700mb, the correlation around the test site has elongated to the west. Another correlation is apparent over the Urals and has extends to the south into the tropics. There appear to be correlations on the edge of the data that would also extend into the tropics in the Pacific off the coast of China. At 500mb the area over the Pacific continues to extend to the west and the area over the Urals is more localized. In the spring, the area of spatial correlation is smaller at the surface than in the winter and there are no longer any other correlations apparent (Fig. 15). At 700mb and 500mb levels the area exhibits a slight east-west elongation and a second area is apparent in northern Canada. The fall correlation area is not significantly different from the spring case at the surface (Fig. 16). At 700mb, it is tighter and exhibits elongation to the east. Another area in the 700mb level is over Siberia and a third over Alaska. At 500mb, these correlation areas are still visible. The area over Alaska is more organized than at 700mb and the area over Siberia is larger. In the summer, the surface spatial correlation exhibits areas over the United States southeast, in the tropics off the west of Africa and off the coast of China(Fig. 17). The 700mb, as in every summer case,is very disorganized and at 500mb the test site elongates to the west onto the North American continent. The 500mb

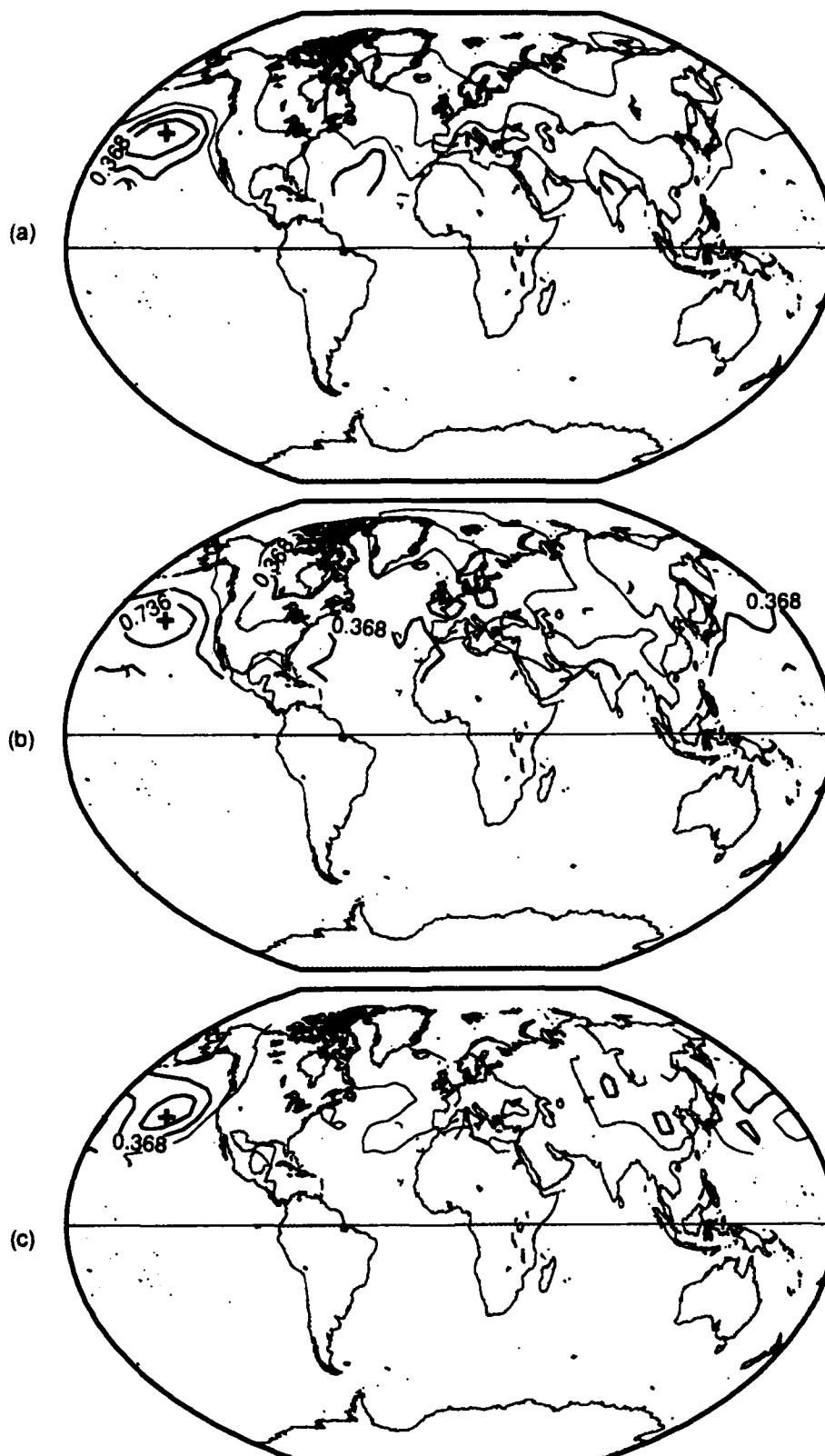


FIG. 13. Spatial correlation of summer temperatures over the Pacific Ocean. (a) 500mb data at 210°E, 40°N for 1964 to 1988. (b) 700mb data at the same point for the same time. (c) Surface data at 212.5°E, 37.5°N for 1950 to 1989.

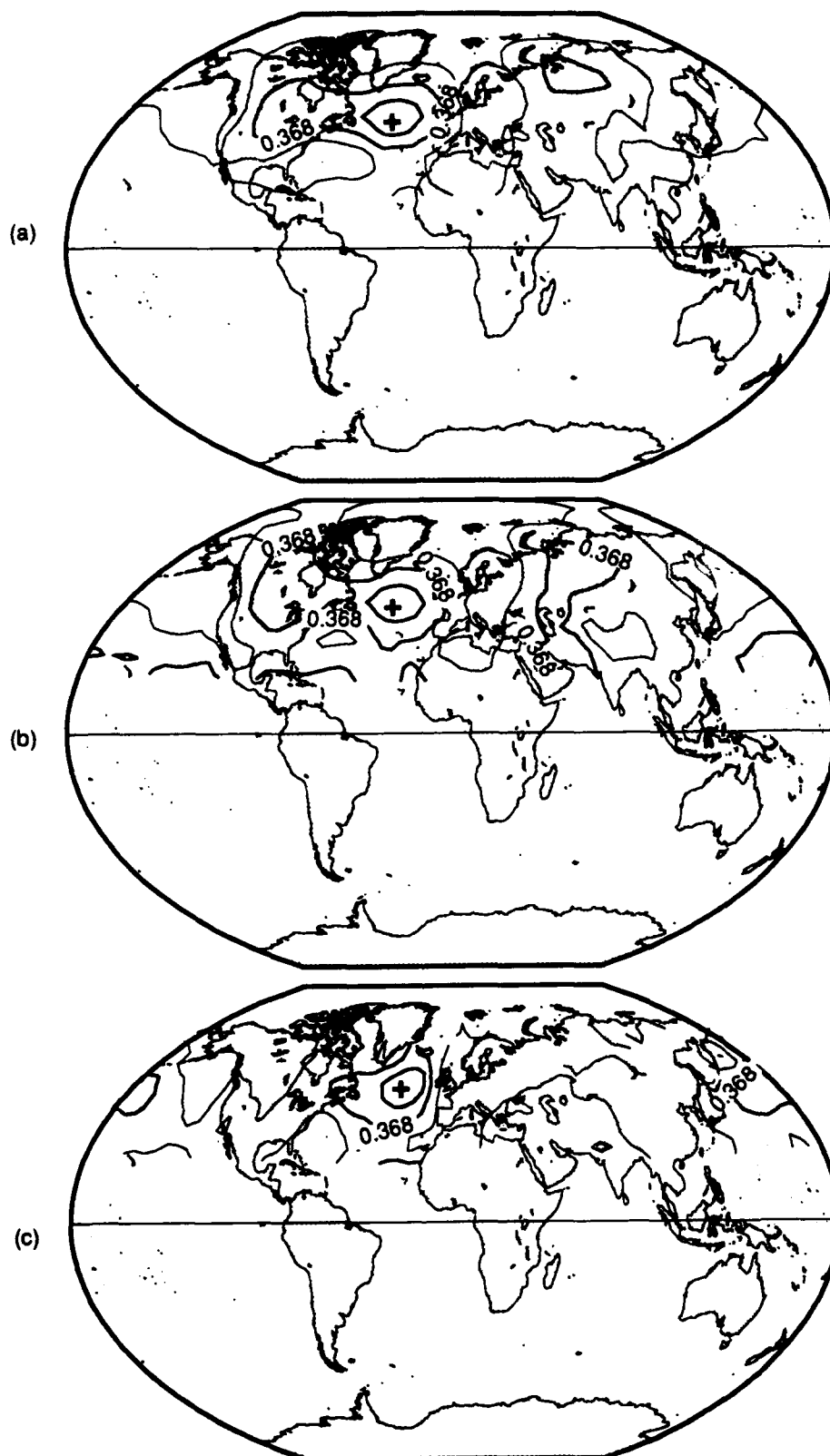


FIG. 14. Spatial correlation of winter temperatures over the Atlantic Ocean. (a) 500mb data at 330°E, 50°N for 1964 to 1988. (b) 700mb data at the same point for the same time. (c) Surface data at 332.5°E, 52.5°N for 1950-1989.

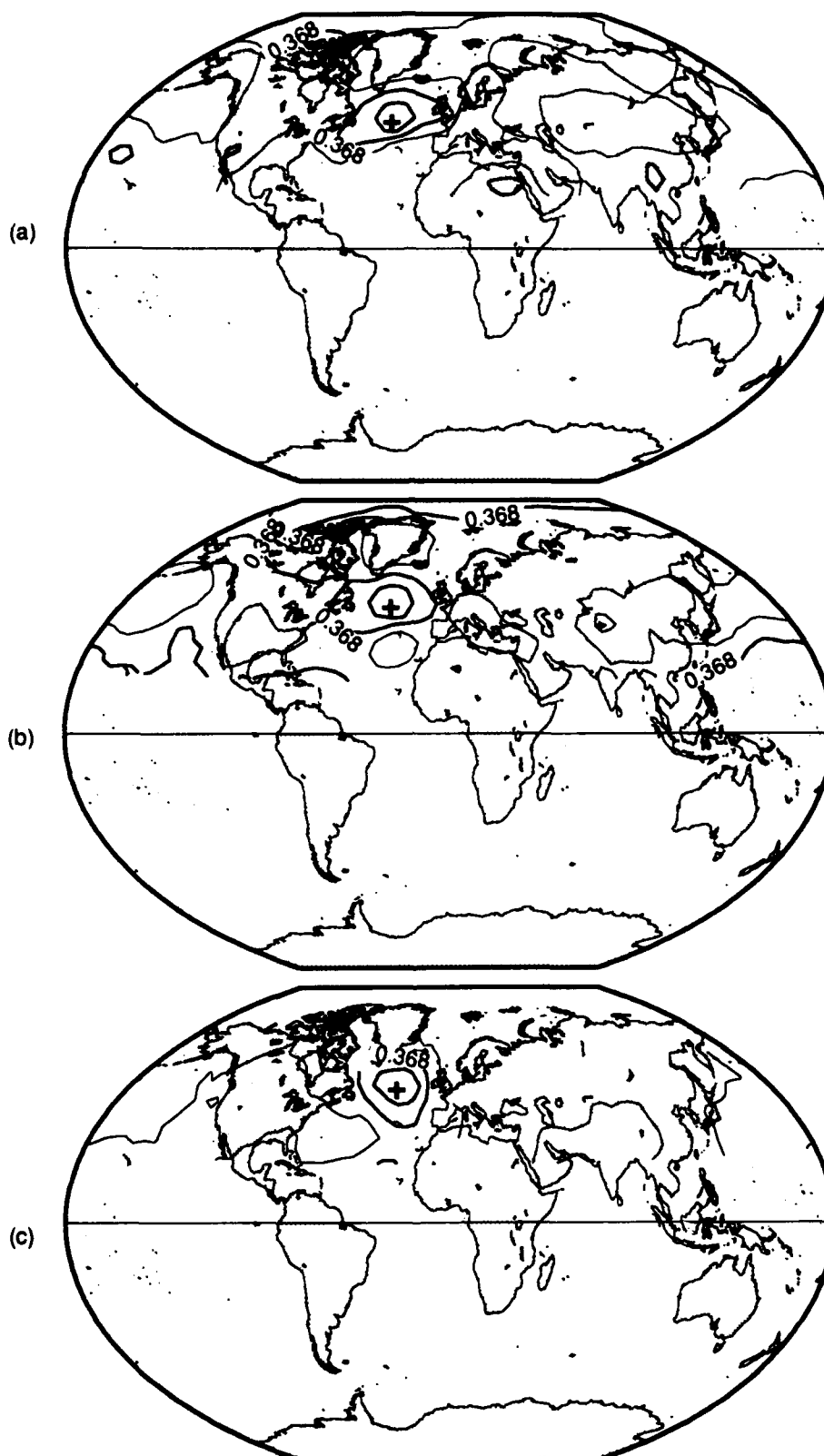


FIG. 15. Spatial correlation of spring temperatures over the Atlantic Ocean. (a) 500mb data at 330°E, 50°N for 1964 to 1988. (b) 700mb data at the same point for the same time. (c) Surface data at 332.5°E, 52.5°N for 1950-1989.

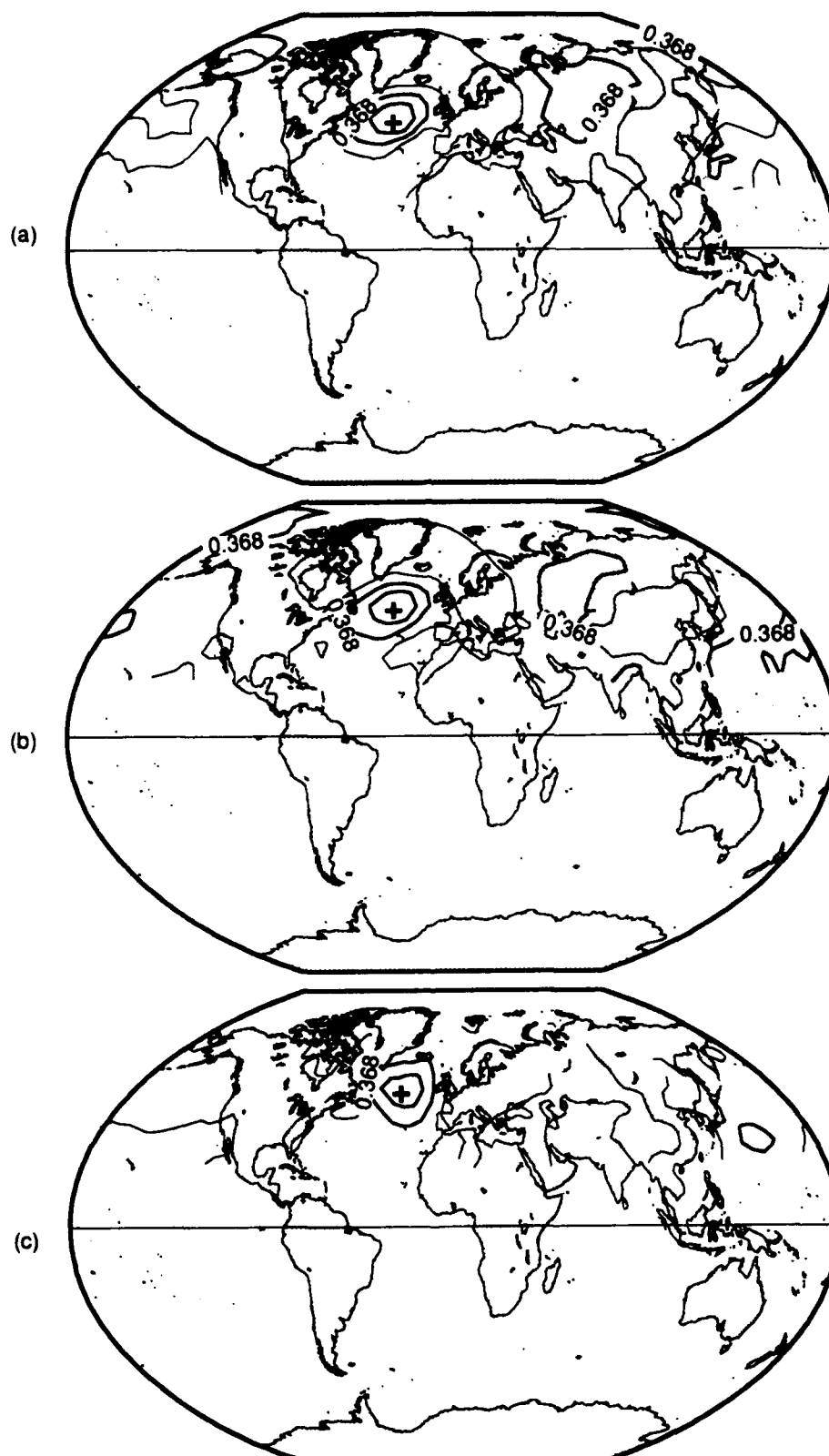


FIG. 16. Spatial correlation of fall temperatures over the Atlantic Ocean. (a) 500mb data at 330°E, 50°N for 1964 to 1988. (b) 700mb data at the same point for the same time. (c) Surface data at 332.5°E, 52.5°N for 1950-1989.

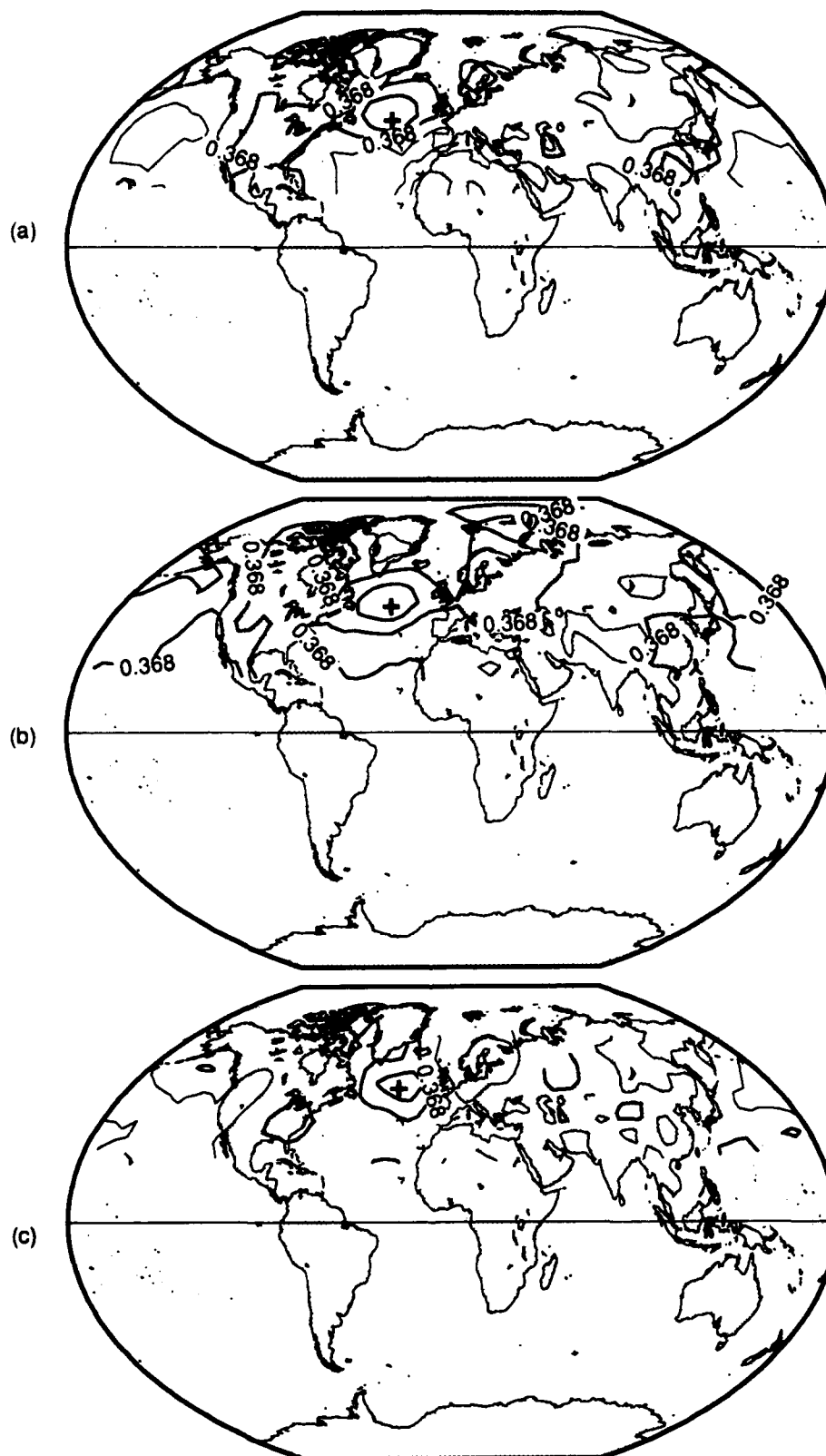


FIG. 17. Spatial correlation of summer temperatures over the Atlantic Ocean. (a) 500mb data at $330^{\circ}\text{E}, 50^{\circ}\text{N}$ for 1964 to 1988. (b) 700mb data at the same point for the same time. (c) Surface data at $332.5^{\circ}\text{E}, 52.5^{\circ}\text{N}$ for 1950-1989.

site elongates to the west onto the North American continent. The 500mb level also exhibits many unorganized areas.

CORRELATIONS BETWEEN VERTICAL LEVELS

Correlations were also calculated between the three levels at each test site. In North America (Fig. 18), the correlations are quite high, ranging between 0.6 and 0.87, in all four seasons. The highest correlation (0.87) occurs in the winter between the surface and 500mb. The fall correlation between the surface and 500mb (0.85) is the next strongest correlation followed by the correlation between the surface and 500mb in the summer. The spring is the only season at this test point that does not have the strongest correlation between the surface and 500mb. The correlations between all three levels in the winter and the spring are not significantly different from each other. In the winter the correlations range from 0.81 to 0.87 and in the spring the correlations range from 0.72 to 0.78. In the summer and the fall, the correlation between the surface and 700mb is much lower than the correlations between the surface and 500mb and the 700mb and 500mb levels. These two seasons exhibit correlations that are similar. In the summer the correlation is 0.67 between the surface and 700mb. In the fall, this correlation is 0.6. The summer correlation between the surface and 500mb is 0.83. In the fall, this correlation is 0.85. The correlation between the 700mb and 500mb levels in the summer is 0.73. This correlation is 0.78 in the fall.

In the area of the Siberian test site the correlations are the stronger in the winter for all three levels (Fig. 19). In the winter the correlation between the surface and the 700mb level is 0.34. In the other seasons, the correlation between these two levels are not significantly different from 0 and range from

	Winter (DJF)	Spring (MAM)	Summer (JJA)	Fall (SON)
Sfc-700mb	0.81	0.78	0.67	0.6
Sfc-500mb	0.87	0.72	0.83	0.85
700mb-500mb	0.81	0.76	0.73	0.78

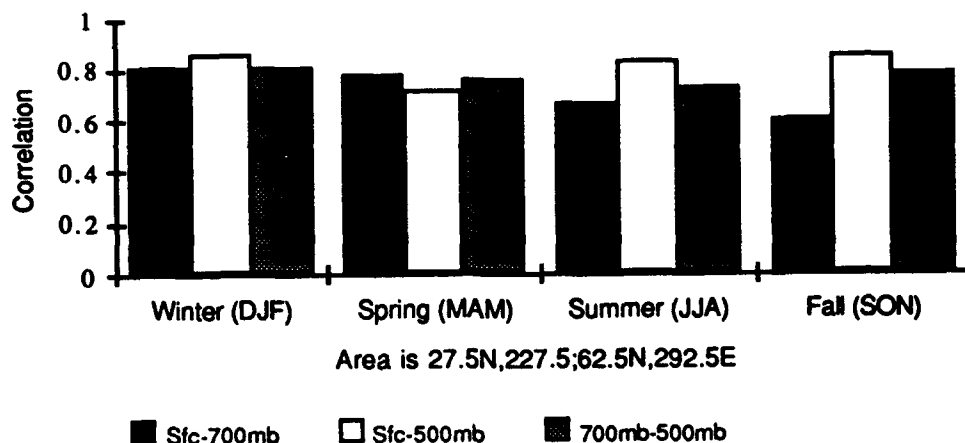


FIG. 18. Vertical correlations over North America

	Winter (DJF)	Spring (MAM)	Summer (JJA)	Fall (SON)
Sfc-700mb	0.34	-0.05	-0.07	-0.06
Sfc-500mb	0.46	0.09	0	0.08
700mb-500mb	0.87	0.33	0.49	0.77

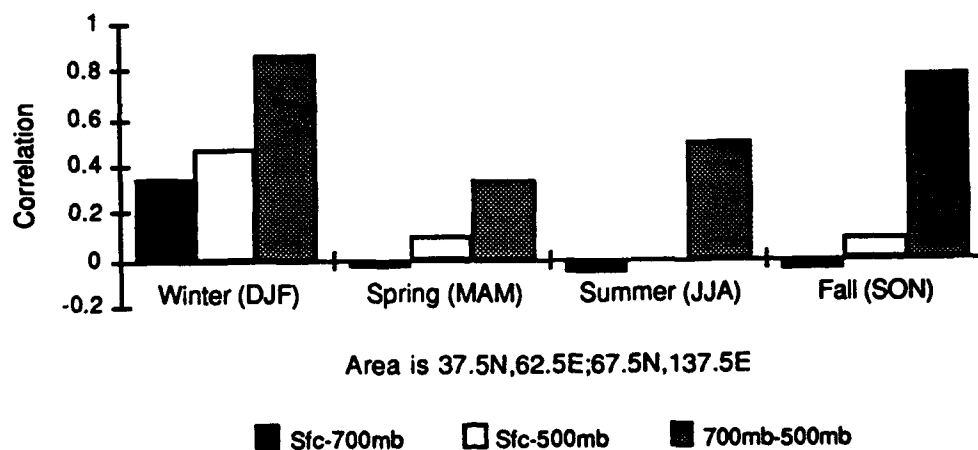


FIG. 19. Vertical correlations over Siberia

-0.07 to -0.05. In the winter the correlation between the surface and the 500mb level is 0.46. Again the the correlation between these two levels is not significantly different than zero for the other seasons, ranging from 0 to 0.09. The correlation between the 700mb and 500mb levels is significant for all four seasons. It is strongest in the winter (0.87), followed by the fall (0.77) , the summer (0.49) and the spring (0.33).

The first ocean area examined surrounds the test site in the North Pacific. As in the two previous cases, the winter exhibits the strongest correlations (Fig. 20). The strongest overall correlation (0.93) is between the 700mb and 500mb levels in the winter. This is followed by the winter correlations between the surface and 700mb and the surface and 500mb which are equal (0.62). The spring exhibits the next highest correlations. The correlation between the surface and 700mb is 0.57, followed by the correlation between the 700mb and 500mb levels (0.5) and the correlation between the surface and 500mb (0.34). The next highest correlations occur in the fall. The correlation between the two upper levels is 0.53, followed by 0.45 between the surface and 500mb and 0.4 between the surface and 700mb. In the summer the correlation is highest in the surface and 700mb is 0.27, followed by 0.2 between the 700mb and 500mb levels and 0.15 between the surface and 500mb.

The last area surrounds the test site in the North Atlantic (Fig. 21). In all four seasons, the correlation between the surface and 700mb is negative. This is smallest in the spring (-0.05). It becomes increasingly more negative, starting with -0.15 in the winter, -0.27 in the summer and -0.33 in the fall. The

	Winter (DJF)	Spring (MAM)	Summer (JJA)	Fall (SON)
Sfc-700mb	0.62	0.57	0.27	0.4
Sfc-500mb	0.62	0.34	0.15	0.45
700mb-500mb	0.93	0.5	0.2	0.53

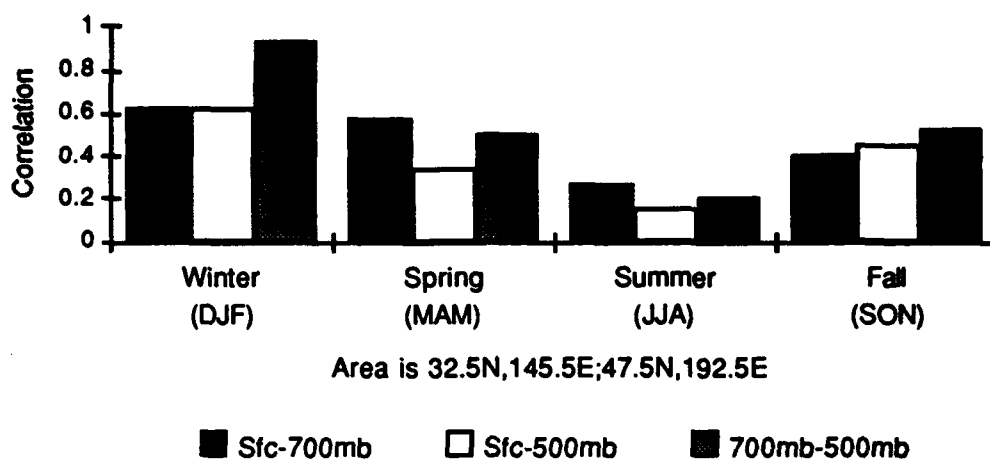


FIG. 20. Vertical correlations over the North Pacific

	Winter (DJF)	Spring (MAM)	Summer (JJA)	Fall (SON)
Sfc-700mb	-0.15	-0.05	-0.27	-0.33
Sfc-500mb	0.13	0.07	0.22	0.25
700mb-500mb	0.83	0.2	0.23	0.31

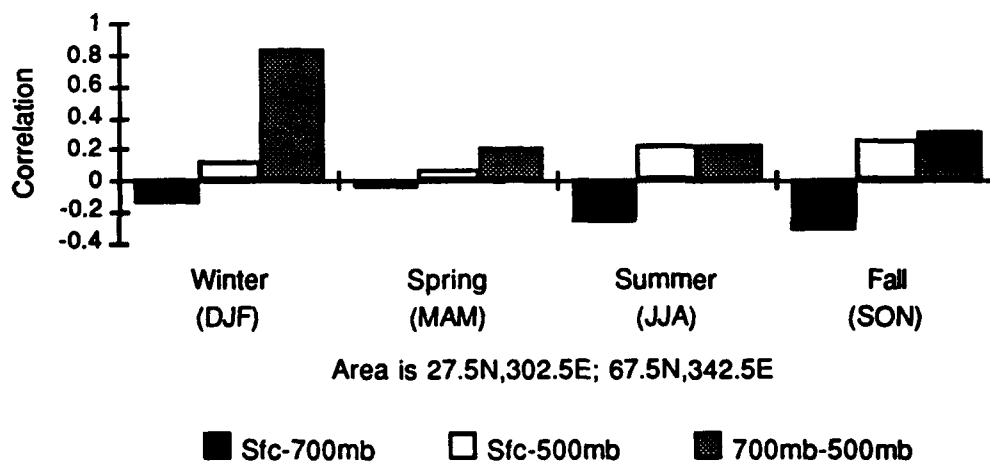


FIG. 21. Vertical correlations over the North Atlantic

correlation between the surface and 500mb is strongest in the fall at 0.25, followed by 0.22 in the summer, 0.13 in the winter and 0.07 in the spring. The strongest correlation for this test site is 0.83 and occurs between the 700mb and 500mb levels in the winter. No other correlation comes close to this value. The next strongest correlation between the upper levels occurs in the fall but is much lower at 0.31, followed by 0.23 in the summer and 0.2 in the spring.

VARIANCE

The variance of the surface temperature at the surface, 700mb and 500mb levels is the next statistic examined. The variability over the land is roughly 4-6 times larger than over the oceans during the winter seasons and 2-3 times larger than on the yearly scale. This result is partially explained by the fact that SST is only a moderately good estimate of air temperature over the ocean. Since the ratio of land area to sea area between the latitudes 20 and 90°N is very large, greater than 0.80, the variability of the land dominates the variance statistics (Barnett, 1978).

In the winter, the variance of surface temperature is confined to the landmasses and is the strongest of all the seasons. In the upper levels, the variance is weak with a bullseye over the Tibetan Plateau at 700mb that is just a result of the higher surface elevations in this area (Fig. 22).

The variance of surface temperature in the spring is confined to the landmasses in the Northern Hemisphere, except across the Bering Strait and is much weaker than the winter surface variance (Fig. 23). At 700mb, the values of the variance are much larger, on the order of 10 times larger, than they were either at the surface or than they were in the winter with a maximum over Siberia and a smaller maximum over Canada. At 700mb, the variance is not confined to the land masses, but seems to exhibit a wave pattern. The same is true at 500mb. At 500mb the variance are still much larger than at the surface, but smaller than at 700mb. The maximums are still apparent over North America and Siberia.

At the surface for the fall season the variance is again confined to the

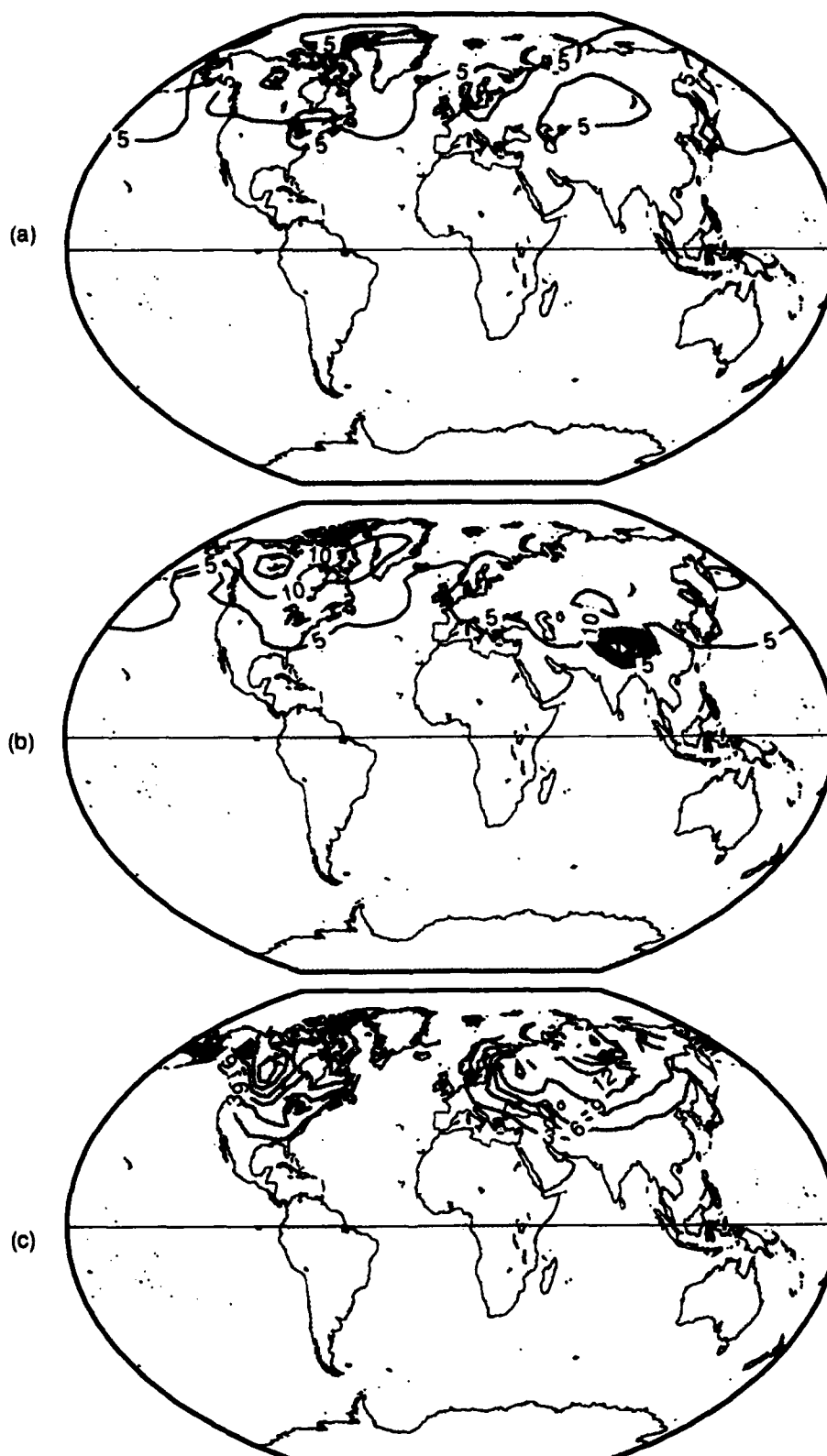


FIG. 22. Variance of winter temperatures. (a) 500mb data for 1964 to 1988. (b) 700mb data for 1964 to 1988. (c) Surface data for 1950 to 1989.

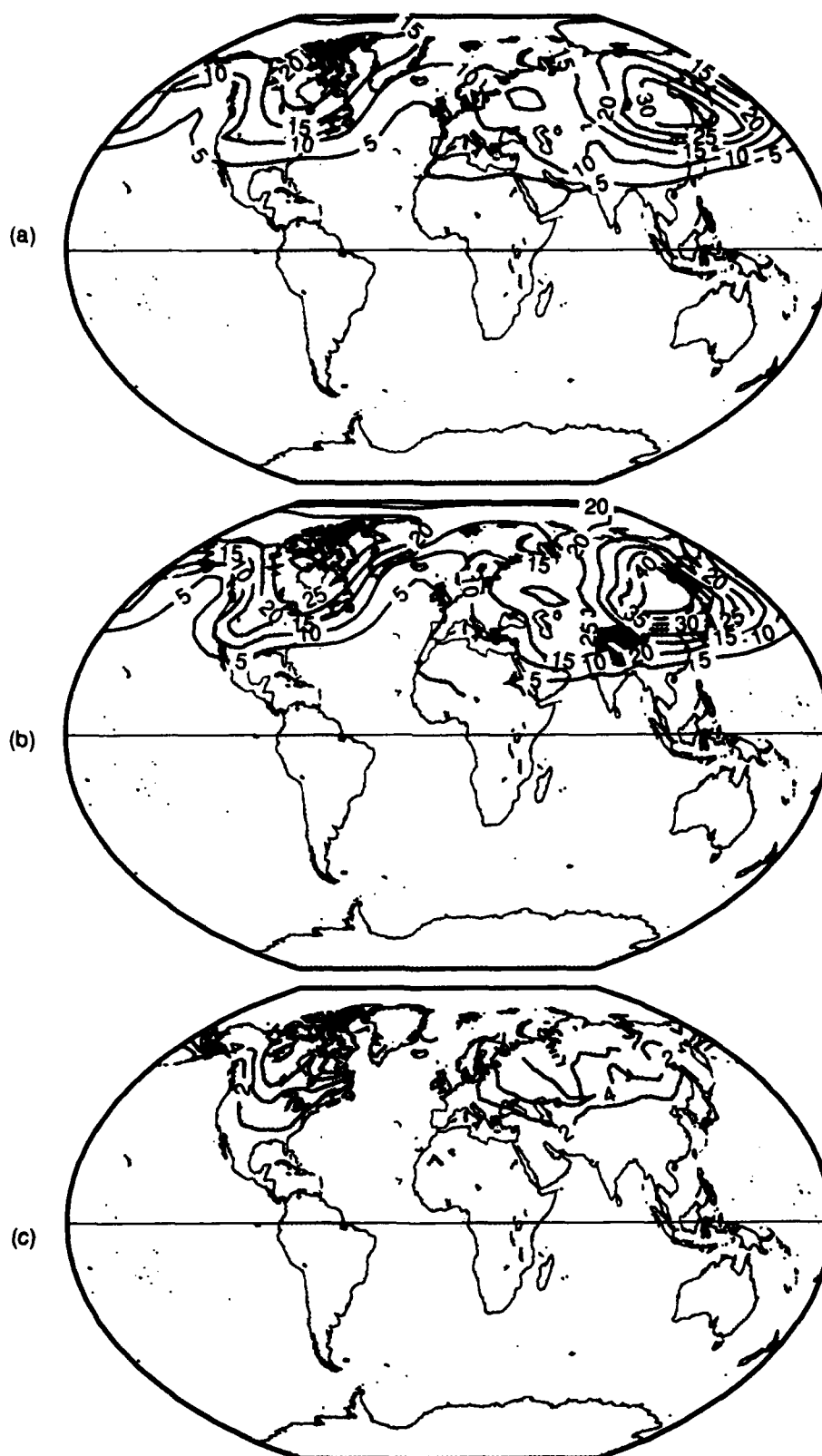


FIG. 23. Variance of spring temperatures. (a) 500mb data for 1964 to 1988. (b) 700mb data for 1964 to 1988. (c) Surface data for 1950 to 1989.

landmasses and is slightly weaker than in the spring (Fig. 24). At 700mb, the variance is no longer confined to the landmasses with maximums located over North America and Siberia. In the fall, the values of the variance over Siberia and over North America at 700mb is larger than in the spring. Once again, the variance of the 500mb level is smaller than at 700mb. The variance is again larger than in the spring over Siberia. Over North America, the variance is smaller and the maximum in the variance is west of the maximum in the spring.

The summer is the least variable season, and that is exhibited in the variance (Fig. 25). There is no significant variance at the surface. At 700mb there is an unorganized pattern of waves with magnitudes 10 times smaller than in the two previous seasons. This is also the case at 500mb.

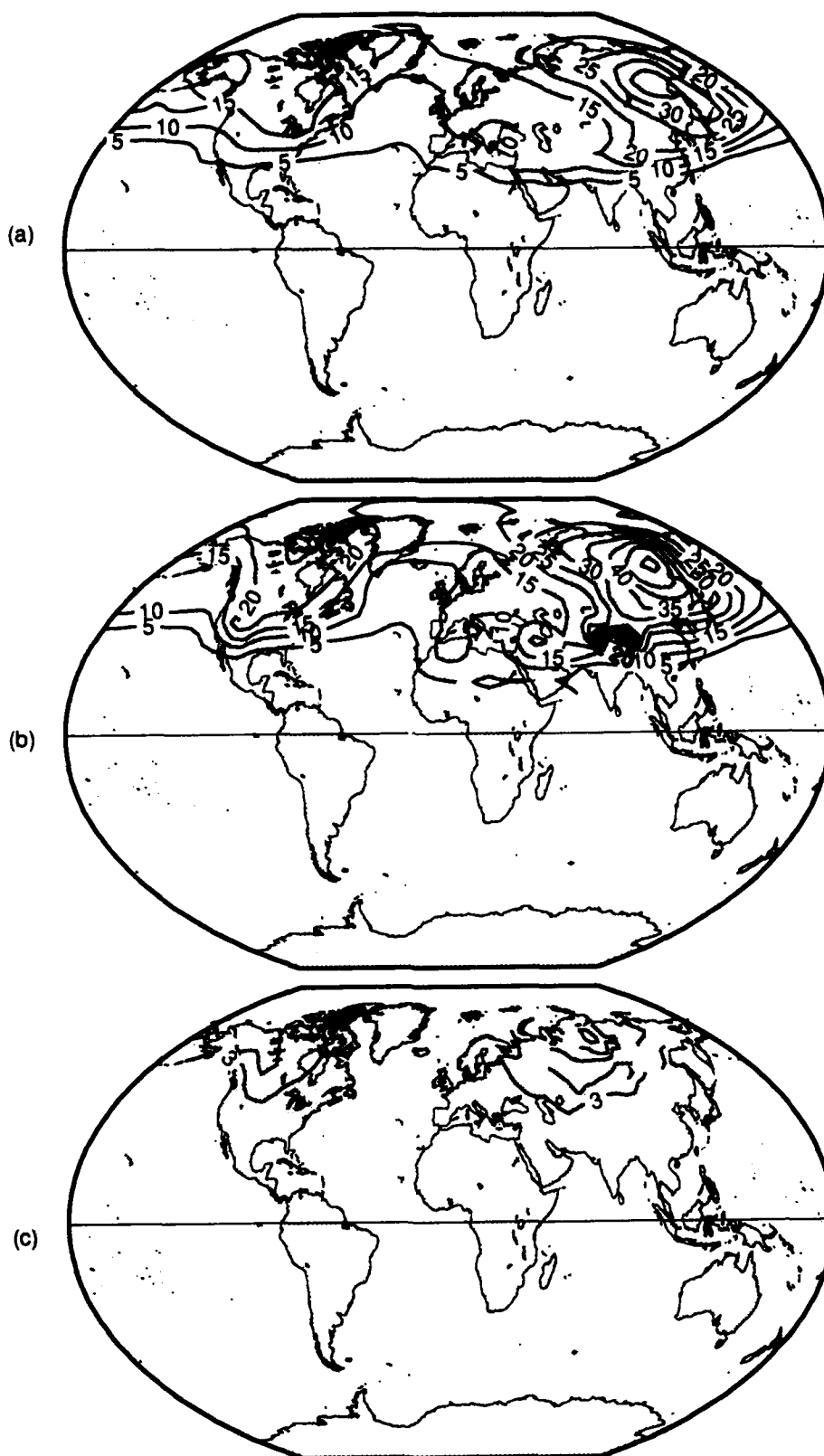


FIG. 24. Variance of fall temperatures. (a) 500mb data for 1964 to 1988. (b) 700mb data for 1964 to 1988. (c) Surface data for 1950 to 1989.

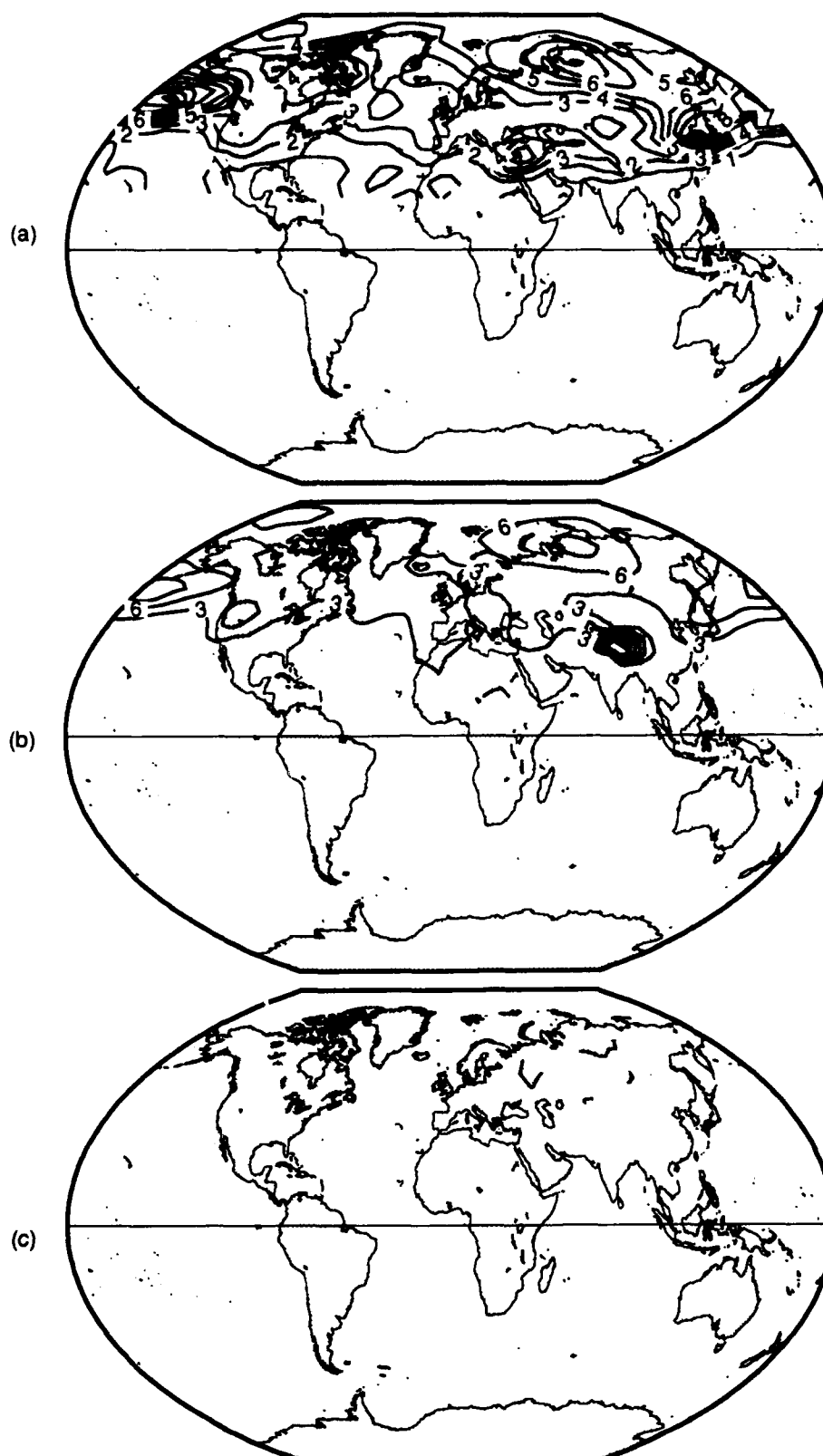


FIG. 25. Variance of summer temperatures. (a) 500mb data for 1964 to 1988. (b) 700mb data for 1964 to 1988. (c) Surface data for 1950 to 1989.

CONCLUSIONS

It has been shown that the variability of monthly averaged temperature field is largest in the winter, followed by the spring, the fall and finally the summer. In almost every instance examined this is the case. In North America, however, the largest variability of spatial correlation is exhibited in the fall. This is related to the differing heat capacities of land and ocean surfaces. Though the winter hemisphere has the strongest variance, there is considerable variation at every point over the hemisphere. The differing effective heat capacities of land and ocean surfaces and the ability of the ocean to transfer energy much more effectively in the vertical causes the annual cycle in the lower tropospheric temperature over land to be advanced in phase by several weeks relative to the timing of transition seasons. The lower tropospheric temperatures over the continents tend to be cooler than those over the surrounding oceans in the autumn and this is reflected in the higher variability at these points.

There are many differences between the test site in North America and the test site in Siberia. The North American continent is small enough that the oceans on each coast impact the continental weather patterns at the month time scale. The oceans warm more slowly in the warm seasons and cool more slowly in the fall and winter seasons than the continent and this limits the correlation extent of the surface temperatures. The generally westerly flow across the Rocky Mountains has an orographic impact that results in a cyclogenesis maximum in the winter and a smaller maximum in the summer. In every season, the Rocky Mountains provide the western

boundary of the North American test site. The Eurasian continent is much larger than the North American continent and the Siberian test site is not immediately bounded by two coasts. The Eurasian continent does not provide the same orographic influences as the North American continent. The largest mountain range is east-west oriented and doesn't interact in the same way with the westerly flow (Palmén and Newton, 1969). As a result, the area of spatial correlation in Siberia is much larger than the correlation over the North American continent. A second result, related to the orographic influence of the Eurasian continent is the fact that the difference between the winter correlation pattern and the summer correlation pattern is larger over Siberia than at any other test site.

In every case, the fall and winter patterns were the most similar. The transition seasons of spring and fall did not exhibit similar patterns. The conventional meteorological seasons studied here, though delayed by about 24 days relative to the solar calendar, occur in the Northern Hemisphere about two weeks earlier than the transition seasons as defined by the tropospheric mean temperature. Temperature exhibits large summer/winter contrasts, and the differences between spring and autumn temperature means are very sensitive to the definition of the seasons. The conventional spring season tends to be colder and to have a stronger tropospheric jetstream than the autumn season due to the projection of the warm/cold season onto the autumn/spring differences. A number of different factors may contribute to the differences between the spring and autumn climates. The most obvious is the phase lag of the annual temperature cycle over the sea

relative to that over land at mid-latitudes, resulting in land temperatures being warmer, relative to sea-surface temperatures, during the spring transition season than at comparable dates during the autumn transition season. A related effect with important consequences for the climate is the relatively lower static stability over the land masses during the spring than during the autumn. This is a direct result of the fact that the land masses warm in spring and cool in autumn more rapidly than the overlying atmosphere, which has a substantial thermal inertia of its own and is influenced by the even larger thermal inertia of the oceans (Fleming et al., 1987).

It is interesting to note that the fall correlation patterns related to the North American test site and the Siberian test site are essentially the same. During the winter, the correlation patterns related to the North American test site and the North Pacific test site are also very similar at the 700mb and 500mb level. This may lead one to assume that there are relationships between temperatures at different points in the Northern Hemisphere and that temperatures exhibit "teleconnections." It is more likely that these apparent relationships are the result of sampling error since we only had 40 years of surface data and 25 years of upper air data. No real statement can be made about these relationships without further investigation. It has to be mentioned that a spatial correlation was also computed over North America 5° south of the test site. Moving the test site in this way caused the other areas of correlation in the Northern Hemisphere to disappear. The fall correlation associated with the Siberian test site exhibits a small correlation at all three levels over the United Kingdom. The North Pacific test site also

exhibits a fairly well organized area over the Ural Mountains. Moving of these two test sites may result in a strong relationship similar to the connection between the other two sites.

Winter in the midlatitudes has the highest baroclinic instability, which is associated with vertical shear of the mean flow and the fact that winter has the strongest horizontal temperature gradient of all the seasons, which must exist to provide thermal wind balance (Holton, 1992). Because winter is so active, it is probably just by chance that patterns in the mid-latitudes may be the same for different test sites in the mid-troposphere. In the winter, spring and fall, the correlation areas at 700mb and 500mb elongate in the east-west direction. This would be expected, as the 700mb level is located above the effects of any orographic influences and the 500mb level is affected by the stronger winds of the polar jetstream. The summer, at all four test sites, is very unorganized at the 700mb level.

These results show that the length scale of the correlation statistics does exhibit a seasonal dependence, but that it is also impacted by other factors such as orography and the proximity of oceans. The next steps in an estimation program to assess the importance of these effects will be to develop the appropriate cyclostationary framework and then to compute the empirical orthogonal functions (Kim and North, 1993; Shen et al., 1994). Other members of the Climate System Research Program (CSRP) are presently at work on this aspect of the project.

The vertical correlations of month averages at these four test sites provide interesting results. North America exhibits large correlations between all three levels for every season. Over Siberia the correlations

between the surface and 700mb and between the surface and 500mb are insignificant, except during the winter. The correlation between the upper levels is largest in the winter, followed by the fall, the summer and the spring. The correlations over the North Pacific are strongest between all levels during the winter. Once again, the correlation between the upper levels is largest in the winter, followed by the fall, the summer and the spring. The correlations over the North Atlantic are insignificant everywhere except between the upper levels during the winter season. These vertical correlations result in a barotropic atmosphere over North America on a monthly time scale and baroclinic atmospheres over the other test sites.

Hsu and Wallace (1985) analyzed the wintertime Northern Hemisphere, 5-day mean sea level pressure field to investigate the possibility that highly baroclinic structures play an important role in low frequency variability using orthogonal principal component analysis and found five modes. Two of these modes can be identified with the North Atlantic Oscillation and the Pacific North American teleconnections and exhibit equivalent barotropic vertical structures. The other three modes include a spatial pattern centered slightly to the north of the climatological Siberian High which covers most of northeastern Asia, a spatial pattern over Asia that consists mainly of a single cell centered over central China, poleward of the Himalayas and a third spatial pattern that is characterized by a dipole over the Pacific Ocean with the northern cell centered over Alaska and extending across the Northern Rocky Mountains. These three patterns are baroclinic.

If one compares these five modes to the test sites addressed in this paper the North Pacific test site is associated with the dipole over the Pacific, the Siberian test site is associated with the spatial patterns over Siberia and the North American test site is associated with the Pacific North American pattern. The Pacific and Siberian test sites are baroclinic which is in agreement with the above results and the North American test site is barotropic which is in agreement with the Pacific North American pattern. The component in the Hsu and Wallace paper that could be associated with the Atlantic test site is equivalent barotropic but is also to the north of the test site which exhibits a baroclinic pattern.

As would be expected, the variance of the monthly averaged surface temperature field is strongest in the winter. The variance of the surface temperature field in the spring and the fall are comparable to one another. In the summer the surface temperature field exhibits virtually no variance. At 700mb, the variance is strongest during the fall and not significantly weaker in the spring. The 700mb variance is weakest during the winter, in direct contrast with the surface patterns. In all four seasons a bullseye is apparent over the Tibetan plateau, in response to the elevated surface. The variance at 500mb is again weakest in the winter. The spring and fall are of comparative strengths to one another. The higher variability at the upper levels during the spring and fall is a result of the transition seasons increased longwave numbers.

Knowledge of how the correlation statistics of temperature fields behave is important in the various climate estimation problems which include

statistical prediction, parameter estimation and signal detection. Expansion of this information to space as well as time will be beneficial to these estimation procedures by adding pattern discrimination to the signal processing algorithms. The surface temperature field is of paramount importance because it is one of the longest time series available for climate studies, and record length is a crucial limiting feature in all statistical estimation schemes. Though there is less upper air temperature information available, comparison of how the upper air fields behave to how the surface temperature fields behave can also lead to important inferences about climate.

REFERENCES

- Barnett, T. P., 1978: Estimating variability of surface air temperature in the northern hemisphere. *Mon. Wea. Rev.*, **106**, 1353-1367.
- Barry, R. G. and R. J. Chorley, 1982: *Atmosphere, Weather and Climate*, 5th ed. Methuen & Co. Ltd., 460 pp.
- Fleming, E. L., G. Lim and J. M. Wallace, 1987: Differences between the spring and autumn circulation of the northern hemisphere. *J. Atmos. Sci.*, **44**, 1266-1286.
- Folland, C. K., T. R. Karl and K. Ya. Vinnikov, 1990: Observed climate variations and change. *Climate Change: The IPCC Scientific Assessment*, Cambridge University Press, 201-238.
- Hansen, J. and S. Lebedeff, 1987: Global trends of measured surface air temperature. *J. Geophysical Res.*, **92**, 13,345-13,372.
- Hardin, J. and R. Upson, 1993: Optimal weighting for point gauges in the estimation of global average temperature. *J. Geophysical Res.*, **98**, 23,275-23,282.
- Hess, S. L., 1959. *Introduction To Theoretical Meteorology*, 2nd Ed., Kreiger Publishing Co., 362 pp.
- Holton, J. R., 1992. *An Introduction To Dynamic Meteorology*, 3rd Ed., Academic Press, Inc., 511 pp.
- Hsu, H. H. and J. M. Wallace, 1985: Vertical structure of wintertime teleconnection patterns. *J. Atmos. Sci.*, **42**, 1693-1710.
- Jones, P. D., 1988: Hemispheric surface air temperature variations: Recent trends and an update to 1987. *J. Climate*, **1**, 654-660.
- Jones, P. D. and R. S. Bradley, 1992: Variations in the longest instrumental records. *Climate Since AD 1500*, Routledge, Chapman & Hall, Inc., 246-268.

Jones, P. D. and K. R. Briffa, 1992: Global surface air temperature variations during the twentieth century: Part 1, spatial, temporal and seasonal details. *The Holocene*, **2**, 165-179.

Jones, P. D. and T. M. L. Wigley, 1990: Global warming trends. *Scientific American*, **263**, 84-91.

Jones, P. D., T. M. L. Wigley and G. Farmer, 1991: Marine and land temperature data sets: A comparison and a look at recent trends. *Greenhouse-gas-induced Climatic Change*, Elsevier Science Publishing Co., 615 pp.

Jones, P. D., S. C. B. Raper, R. S. Bradley, H. F. Diaz, P. M. Kelly, and T. M. L. Wigley, 1986: Northern hemisphere surface temperature variation: 1851-1984. *J. Clim. Ap. Meteorol.*, **25**, 1213-1230.

Kim, K. Y. and G. R. North, 1993: EOF analysis of surface temperature field in a stochastic climate model. *J. Climate*, **6**, 1681-1690.

Kim, K. Y. and G. R. North, 1991: Surface temperature fluctuations in a stochastic climate model. *J. Geophysical Res.*, **96**, 18,573-18,580.

North, G. R. and R. Calahan, 1982: Predictability in a solvable stochastic climate model. *J. Atmos. Sci.*, **38**, 504-513.

Palmén, E. and C. W. Newton. 1969. *Atmospheric Circulation Systems: Their Structure and Physical Interpretation*. Academic Press, 603 pp.

Shen, S. S. P., G. R. North and K. Y. Kim, 1994: Spectral approach to optimal estimation of the global average temperature. *J. Climate*, in press.

VITA

Bridget Frances Tobin was born on August 18, 1967 in St. Louis and lived in the state of Missouri until 1985. After graduating from Hermann Highschool in Hermann, Missouri in 1985, she enrolled at Creighton University in Omaha, Nebraska, where, in 1989, she received a Bachelor of Science degree in atmospheric science. In May of 1989 she was commissioned as a second lieutenant in the United States Air Force and was assigned to the 443rd Military Airlift Wing as the Wing Weather Officer at Altus Air Force Base, Oklahoma from October 1989 to July 1992. From August 1990 to March 1991 she was assigned to the 1701st Strategic Wing in Jeddah, Saudi Arabia as the Weather Detachment Commander. She was accepted as a graduate student at Texas A&M in 1992 and did research for Dr. Gerald R. North.

Bridget can be contacted through Martha Kirchoff, Department of Meteorology (CSRP).